Atmospheric Research 274 (2022) 106201

Contents lists available at ScienceDirect

Atmospheric Research

journal homepage: www.elsevier.com/locate/atmosres

Regional modulating behavior of Indian summer monsoon rainfall in context of spatio-temporal variation of drought and flood events

Shruti Verma [a], R. Bhatla [a,b,*], N.K. Shahi [c], R.K. Mall [b]

[a] Department of Geophysics, Institute of Science, Banaras Hindu University, Varanasi, India
[b] DST-Mahamana Centre of Excellence in Climate Change Research, Institute of Environment and Sustainable, Development, Banaras Hindu University, Varanasi, India
[c] Centro Euro-Mediterraneo sui Cambiamenti Climatici (CMCC), Bologna, Italy

ARTICLE INFO

Keywords:
SA-CORDEX
Regional climate model
Flood
Drought
Empirical orthogonal function

ABSTRACT

In this paper, daily modulating behaviors of Indian summer monsoon rainfall (ISMR) has been evaluated over eight important sub-zones of India viz Northwest India (NWI); Northcentral India (NCI); West Peninsular India (WPI); Eastern Peninsular India (EPI); Southern Peninsular India (SoPI); Central India (CI), Northeast India (NEI) and Western Ghat (WG) using latest SA-CORDEX simulated climate data during 1981–2015. The climate extreme indices, standardized precipitation index (SPI) and empirical orthogonal function (EOF) have been utilized to uncover substantial regional spatial patterns and temporal variability of monsoon precipitation over India and its sub regions to understand the regional modulation of these events based on duration, frequency and severity. The comprehensive assessment of ISMR modulated characteristics (intensity, spell, and frequency) were showing significant decreasing trend over NEI and NCI which can be leading factors for demarcating major hotspots for land degradation, effective management and adaptation towards water resources and hazards related to the flood/drought events. India has received flood events (1983, 1988, 1994, 2005, 2011, 2013) and drought event (1982, 1987, 2002, 2004 and 2009) during 1981–2015, which have been verified with SA-CORDEX RCMs (RegCM4.7, COSMO & REMO2015) using SPI. The first mode of EOF(IMD), explained 17% of the total SPI variability on the interannual scale, shows anomalous large positive values concentrated over the western peninsular region and extending towards central India as well as the NWI region of India. On the other hand, high anomalous negative values dominated over the NEI and eastern parts of the Indo-Gangetic Plain. Therefore, this study underscores the importance to uncover the prevalent dynamics and climate change variability on changing trend variability of the precipitation indices, drought and flood characteristics. As moderate to severe drought variability portrays a diversity over regional scale viz northwest India, north central India, eastern ghat of the southern peninsular region and northeast India while the occurrence of moderate to severe flood are dominated towards Himalaya region (26°N-35°N; 70°E-80°E), western peninsular region and western ghat.

1. Introduction

The prediction of occurrence, intensity and location of weather/climate condition still is challenging task using numerical weather prediction. The Indian summer monsoon contributing 80% of the total annual precipitation of the country which is showing phase alteration with frequent severe to moderate drought and flood episodes due to climate change. In the climate changing scenario, regional climate modulation would cause more devastating effects on the society, causing human loss, degrading natural resources, indirectly affects the ground water resources and cause huge economic loss. The vagaries in the regional temperature and precipitation are triggered by different anthropogenic activities such as greenhouse gas emissions and land use changes in the past century (Bindoff et al., 2013; Sarojini et al., 2016; Varikoden and Revadekar, 2020). Global warming directly impacts regional precipitation, by increasing evaporation thus surface drying, thereby increasing the intensity and duration of drought (Trenberth, 2011; Allan and Soden, 2008). The potential contribution of El-Nino events in driving the rising correspondence of hot and dry extremes over the Indian subcontinent under the warming climate, which leads us to the increased severity of hot & dry monsoon extremes and possess a substantial challenge to the future food security of India (Mishra et al.,

* Corresponding author at: Department of Geophysics, Institute of Science, Banaras Hindu University, Varanasi, India.
E-mail address: rbhatla@bhu.ac.in (R. Bhatla).

https://doi.org/10.1016/j.atmosres.2022.106201
Received 10 December 2021; Received in revised form 11 March 2022; Accepted 11 April 2022
Available online 18 April 2022

2020a). The notable decreasing trend over the Indo Gangetic plain (IGP) and the western Ghat (WG) has been observed during the Indian summer monsoon which is around 6% from 1951 to 2015 (Krishnan et al., 2020). Roxy et al., 2015 highlight the warming in the Indian Ocean potentially weakens the land-sea thermal contrast, which affects the summer monsoon Hadley circulation, therefore decreased monsoon rainfall has been observed over parts of South Asia. Another study of Mishra et al., 2020b studies the El Nino Southern Oscillation (ENSO) as a potential driver of these extreme weather events, undergoes deficient or excess rainfall over a region.

The formation of drought is a slow process it takes months to years to evolve, it can be characterized by three main aspects i.e., intensity, duration and areal extent. In general, the drought phenomenon is classified into four categories viz., meteorological, hydrological, agricultural, and socio-economic based on its nature. The meteorological drought is the introducer of the rest of the three-drought types. Initially, shortage of soil moisture, then a decrease in streamflow which results into a shortage of water storage in reservoirs, depletion of groundwater table and finally a negative impact is shown upon human economy and society (Tsakiris, 2017). The drought and flood severity are measured as the degree of precipitation, soil moisture or water shortage deficit. The occurrence of drought and flood events cause significant damage to agricultural livelihood (Sikka, 1999; Vasiliades et al., 2011; Narasimhan and Srinivasan, 2005; Pai et al., 2017). India has experienced increased occurrence of floods and drought in the recent past (Parthasarathy et al., 1994; Rajeevan et al., 2008; Preethi et al., 2019). One-third of the total landmass of India is semi-arid and arid tropical types that's why India experiencing high vulnerability to frequent drought and desertification (Nagarajan, 2003). The recent article of Christian et al., 2021 categorized 'India' in the list of *flash drought hotspot* in the world. Recently, India has experienced increase in occurrence of flood and drought cases (Parthasarathy et al., 1994; Meehl et al., 2005; Rajeevan et al., 2008; Preethi et al., 2019). The drought of 1987 was the worst drought of the last century, with an overall rainfall deficit of 19% from the normal which experience over all India except Bihar and some parts of North East India (NEI). According to government reports this drought affect nearly 60% of the crop area and more than 85 million people were severely affected. On the other hand, major floods over Bihar (1987) cause major destruction, causing extensive losses and death, due to severe floods due to the overflow of the Koshi river which claimed the loss of lives of 1399 humans, 302 animals, and public property worth US $950 million. There is evidence of increased localized heavy precipitation occurrences in response to increased atmospheric moisture content. Over central India, the frequency of daily precipitation extremes with rainfall intensities exceeding 150 mm per day increased by about 75% during 1950–2015 (Mujumdar et al., 2020). The lowest crop production recorded for the last 50 years was observed in 2002 during the Kharif (March to June) season, and crop loss caused a 1% reduction in the GDP of India. The consecutive drought during 2000–2012 caused a severe loss in crop production. The study of Jena and Azad (2021) highlights all India drought and flood cases using the CMIP5 model and reported frequent occurrence of drought in future climate change scenarios.

Instead, flood is one of the most devastating disasters in India, generally localized with uneven distribution and heavy precipitation during the monsoon period (Dhar and Nandargi, 2003; Mishra et al., 2012). Three consecutive flash floods occurred during 2005 in Mumbai (July), Bangalore (October) (Guhathakurta et al., 2011), Chennai (October and December) (Lavanya, 2021) causing loss of lives. On estimate, the coastal flood risk (~36 million population) in India has been increased significantly (The Hindu, 2019). Every year, floods cause major destruction of Bihar state, causing extensive losses and death, in 1987 experienced severe floods due to the overflow of the Koshi river which claimed the lives of 1399 humans, 302 animals, and public property worth US$950 million. Approx. 8 million hectares of the Indian land area were affected by floods (Ray et al., 2019). However, best of our knowledge there are lacunae in the research based on modulated rainfall characteristics for India along with its sub-regions.

The report of IPCC AR5 indicated the climate change impacts are expected to increase in near as well as in far future. Therefore, the reliable and scientific-based climate information helps in building the resilient future of the country. The simulation of various climate models provides useful information about past, present and future climate. Indian subcontinent adheres to topographical differences such as high mountains of Himalaya and western ghat which affect the regional forcing in global circulation model (GCM) because of their coarse resolutions but on the other hand, regional climate models (RCMs) perform better to capture those local climate properties (Sinha et al., 2013; Dash et al., 2015; Raju et al., 2015; Luo et al., 2018; Mishra and Dwivedi, 2019; Mishra et al., 2020a). The limitation in the representation of regional monsoon in GCM simulation (Sperber et al., 2013; Sylla et al., 2015; Ashfaq et al., 2021) has been reported, therefore the regional and local scale climate simulation still rely on the dynamical downscaling of GCMs with various initial and boundary forcing in RCMs (Giorgi and Gutowski Jr, 2015).

The RCM provides the high-resolution simulation and projection on the climatological timescale (up to 2100 years) (Giorgi and Gutowski Jr, 2015). With the advancement in technology and resources, the spatial resolution of RCMs has been increased. At finer resolution RCM climate data will help in the application studied of agriculture, water management, urban planning, rural development etc. so that demand of high-quality regional climate information has been increasing. The Coordinated output for regional evolutions (CORE) (Gutowski Jr. et al., 2016) was initiated in the framework of World climate research programme (WCRP) as Coordinated regional climate downscaling experiment (CORDEX). Its main objective is to produce a coordinated set of downscaled regional climate information for the different regions of the world at better resolution and quality to support the vulnerability, impact, adaptation and climate service application (Giorgi et al., 2009; Ruane et al., 2016). The CORDEX data enable us to provide detailed regional climate change assessment and its impact. The RCMs REMO and RegCM are the first participating models in the CORDEX CORE ensembles (Jacob et al., 2012; Giorgi et al., 2012; Saeed et al., 2012). It is crucial to evaluate the model performance to estimate the impact of climate change on India and its sub-regions (Kodra et al., 2012). In this study, the extraordinarily high resolution three RCMs simulation (RegCM4.7, COSMO & REMO2015) over the SA-CORDEX domain has been selected to investigate the spatial and temporal dimensions of extreme climate indices along with meteorological droughts and floods over India and subregions in the context of regional modulation index. The major objective of this study to investigate regional variation and changes in the Indian summer monsoon that account for modulation in the amplitude, frequency and duration (regarding length of wet/dry season). Along with this the multi-nature aspect of drought and regionalized flood characteristics; Intensity, frequency, occurrence and spatial distribution to identify hotspot/critical drought and flood-prone areas in the context of regional variability with the help of the Standardized Precipitation Index (SPI). This Index is highlighted by the world meteorological organization (WMO) for the detection of drought and flood cases (Svoboda, 2016) and its spatio temporal variability aspect has been uncovered using Empirical orthogonal function (EOF).

The objectivity of this study defined in to three parts, firstly model validation and study of summer monsoon rainfall variability and its modulated behavior over India and its subregions. In which modulating characteristics of the monsoon rainfall in terms of duration of consecutive dry days and wet days, intensity in term of maximum one day precipitation and mean daily intensity, and lastly the frequency of moderate, wet, very wet and extremely wet days with respect to 75th, 90th, 95th and 99th percentile daily ISMR. Second objective to analyzed spatial-temporal distribution of drought and flood in term of occurrence and severity to highlighted as phase transition/modulation (flood and drought episode) during monsoon rainfall. The main intent of this section is to draw a comprehensive picture of conceivable modulation in

Table 1
Namelist, subregions and domain considered over India.

Namelist		Domain	Climate	Average monsoon rainfall
AI	All India	LON 67°–98°; LAT 6°–38°	Tropical monsoon, tropical wet and dry	88 cm
Subregions of India				
NWI	North west India	LON 72°-79°; LAT 21°-30°	Arid & semi arid low land	64 cm
NCI	North central India	LON 79°-87°; LAT 21°-28°	Humid subtropical	98 cm
WPI	Western peninsular India	LON 73°-78°; LAT 16°-21°	Tropical wet and dry	89 cm
EPI	Eastern peninsular India	LON 78°-84°; LAT 16°-21°	Tropical wet and dry	96 cm
SoPI	Southern peninsular India	LON 75°-80°; LAT 10°-16°	Tropical wet and dry, non-arid climate	61 cm
NEI	North east India	LON 90°-95°; LAT 23°-28°	Humid sub-tropical	156 cm
CI	Central India	LON 72.25°-85°; LAT 21.25°-26.75°	Tropical wet and dry & Humid subtropical	85 cm
WG	Western Ghat	LON 72°-76°; LAT 12°-22°	Tropical wet	131 cm

flood & drought characteristics using observation data (IMD) and RCMs (RegCM4.7, COSMO and REMO) output. Third objective is to find spatio-temporal pattern of year-to-year variability in drought and flood events using EOF. It is assumed that this structure could be separated into orthogonal sub-climate regimes via empirical orthogonal function (EOF) which include analysis on the spatial monsoon SPI to reveal the dominant spatio-temporal patterns of regional drought and flood.

2. Study area, data and methodology

2.1. Study area

The interannual variability and regional modulating behavior of rainfall has been examined in the framework of the spatial and temporal dimension of drought and flood over eight homogenous rainfall zones or subregions of Indian subcontinent. The brief description of rainfall subregion/zones described in Table 1 viz. *North west India (NWI), Northcentral India (NCI), Western peninsular India (WPI), Eastern peninsular India (EPI) and Southern peninsular India (SoPI)* (Bhatla et al., 2019; Verma et al., 2021), based on the changing behaviors of extreme rainfall three important regions i.e. *North east India (NEI), Central India (CI) and Western ghat (WG)* have been updated in this study shown in Fig. 1.

2.2. Data used

In this experiment, the investigation of the reliability of SA-CORDEX RCMs of three high resolution (at 0.22° or 25 km) RCMs (RegCM4.7, COSMO & REMO2015) ERA-Interim-driven simulations of over SA-CORDEX domain has been selected to investigate the spatial and temporal dimensions of extreme climate indices along with meteorological droughts and flood over India and its subregions. A brief model description of all RCMs used in this study given in Table 2. The Abdus Salam International Centre for Theoretical Physics regional climate model RegCM4.7(version 4.7) (Giorgi et al., 2012) developed which is driven by ERA-Interim reanalysis data at a grid spacing of 25 km over the SA-CORDEX domain. The COSMO model (COnsortium for Small scale Modeling) limited-area numerical weather prediction model developed by Deutscher Wetterdienst (DWD) in the 1990s for weather forecasting applications (Baldauf et al., 2011). Within the CORDEX-

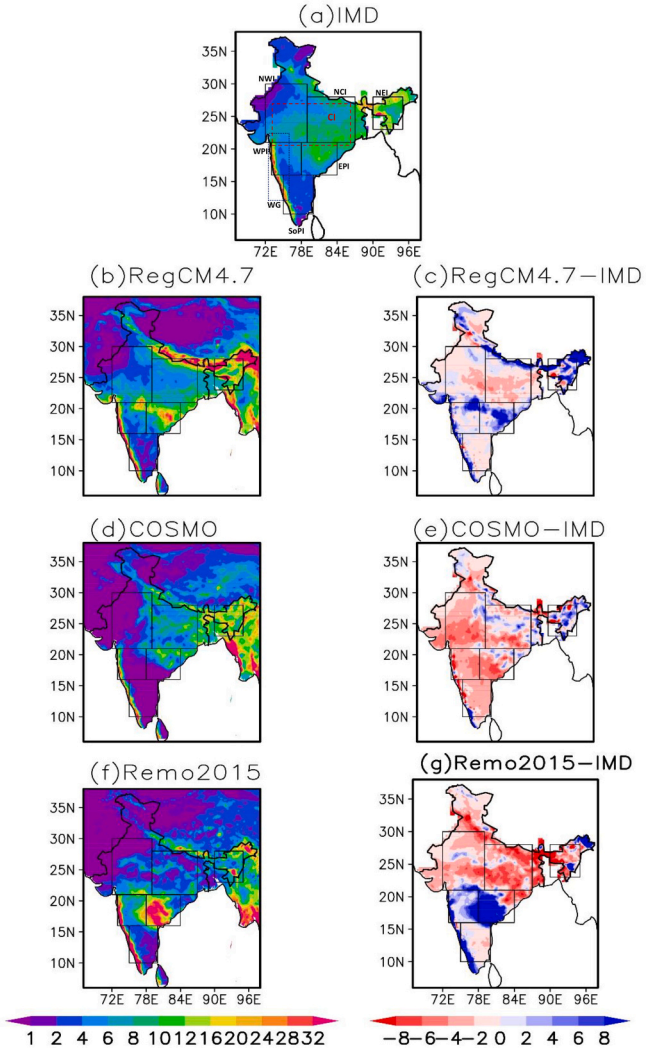

Fig. 1. a-g: Climatological spatial Indian summer monsoon rainfall (mm/day) distribution (first column) and mean bias (Second column) over India and its region during 1981–2015, (a). observation (IMD); (b&c). RegCM4.7; (d&e). COSMO; (f&g). REMO.

CORE framework, COSMO-crCLIM-v1–1 was used at a horizontal grid spacing of 0.22°, including 57 vertical levels and a time step of 150 s, as proposed by Asharaf and Ahrens, 2015 and Sørland et al. (2021). The latest hydrostatic version of REMO (REMO2015) (Remedio et al., 2019) is used with 27 hybrid sigma-pressure coordinate system. The performance of SA-CORDEX rainfall data sets over all selected subregions of India has been compared with gridded daily rainfall (0.25° × 0.25°) data set obtained from India Meteorological Department (IMD) (Rajeevan and Bhate, 2009) consider for south west monsoon (SWM) (June to September) season for the time period of 1981–2015.

2.3. Methodology

2.3.1. Model validation

The RCM evolution SA-CORDEX data are regridded (bilinear interpolation) to the observational grid (0.25° × 0.25°). To compare the spatial rainfall pattern and its variability, climatological mean, interannual variability or standard deviation (SD), mean bias (MB), root mean square error (RMSE) of SWM rainfall at each grid level were calculated for RCM output (RegCM4.7, COSMO, REMO) as well as IMD's observational data during 1981–2015. To evaluate skill in reproducing the spatial pattern of the present-day precipitation pattern, Taylor

Table 2
Model configuration and detailed description of model parameterization:

	RegCM47	COSMO	REMO2015
Institute	ICTP	CLMcom-ETH	GERICS
version	RegCM4-7_v0 (Giorgi et al., 2012)	COSMO-crCLIM-v1–1_v1 (Baldauf et al., 2011)	REMO2015_v1 (Jacob et al., 2012; Remedio et al., 2019)
Dynamics	Hydrostatics		
Model domain	South Asia CORDEX domain (22°S–50°N; 10°E–130°E)	South Asia CORDEX domain (22°S–50°N; 10°E–130°E)	South Asia CORDEX domain (22°S–50°N; 10°E–130°E)
Resolution	25 km horizontal	0.22°	0.22°
Vertical level	23	57	27
PBL	Holtslag PBL (Holtslag et al., 1990)	–	Monin-Obukhov similarity theory (Louis, 1979)
Initial and boundary conditions	ECMWF ERA Interim reanalysis (Dee, 2011)	ECMWF ERA Interim reanalysis (Dee, 2011)	ECMWF ERA Interim reanalysis (Dee, 2011)
Convection	Emanuel over Land & Tiedtke over Ocean	Tiedtke (1989)	Tiedtke (1989)
Microphysics	SUBEX (Pal et al., 2000)	–	Lohmann and Roeckner (1996)
Simulation period	1981–2015	1981–2015	1981–2015

Table 3
Climate indices in term of duration, frequency and intensity.

Index		Characterization	Unit
Duration	CDD	Consecutive dry days (daily rainfall<1 mm)	days
	CWD	Consecutive wet days (daily precipitation≥ 1 mm)	days
Intensity	RX1D	maximum 1-day precipitation amount	mm
	MDI	Mean daily intensity per time period (*Total wet days precipitation divided by the number of wet days)	mm/day
Frequency	RF > 20/HPD	No. of heavy precipitation days (daily precipitation>20 mm)	days
	RF > 25/VHPD	Very heavy precipitation days (daily precipitation>25 mm)	days
	RF75p	Moderate days w.r.t.75th percentile of reference period	mm/day
	RF90p	Wet days w.r.t. 90th percentile of reference period	mm/day
	RF95p	Very wet days w.r.t. 95th percentile of reference period	mm/day
	RF99p	Extremely wet days w.r.t. 99th percentile of reference period	mm/day

diagram (Taylor, 2001) was applied, which provides a concise statistical summary of the degree of correlation (PCC; pattern correlation coefficient), centered root-mean-square error (RMSE) and the ratio of spatial standard deviation (RSD). Along with this, probability density function (PDF) and empirical cumulative distribution function (ECDF) of the daily precipitation intensity have plotted to study the overall distribution of the variable over a region.

2.3.2. Climate Indices

The monitoring, detection and attribution of changes in climate extreme calculated with help of climate indices defined by the Expert Team on Climate Change Detection and Indices (http://etccdi.pacificclimate.org/index.shtml (Karl et al., 1999; Peterson, 2005)); see Table 3 for details. These indices have been widely used in climate change research and are considered as representative for model performance (Zhu et al., 2020). The precipitation indices categorized into duration, intensity and frequency has been analyzed for selected sub-regions of the India, the detailed description of the indices given in Table 3 These indicators include consecutive dry days (CDD), consecutive wet days (CWD); intensity indicators include maximum 1-day precipitation amount (RX1) and mean daily Intensity (MDI); frequency indictor includes number of heavy precipitation days (HPD), number of very heavy precipitation days (VHPD) and categorization of the precipitation event based on 75th, 90th, 95th and 99th percentile viz., moderate, wet, very wet and extremely wet rainfall of the daily ISMR.

2.3.3. Duration, severity and intensity of flood and drought event

For regionalized characterization of duration, severity and intensity of flood and drought event 'SPI' (McKee et al., 1993) was used which is based on the probability of rainfall for selected time period (1981–2015). The duration of flood and drought events reflect its impact on the variability of water resource and storage, soil moisture etc. for the computation of SPI monsoon period (June–September) has been consider over all India and its sub regions. The long time series of rainfall is fitted to probability distribution which then transform into a standardized normal distribution. The classification of the flood intensities has been classified value of SPI (mentioned in Table 5) such as 'Near normal' (0–0.99), 'moderate' (1.0–1.49), 'severe' (1.5–1.99), 'extreme' (above 2.0) similarly drought intensities defined by 'Near normal' (0 to −0.99), 'moderate' (−1.0 to −1.49), 'severe' (−1.5 to −1.99), 'extreme'(below −2.0). In order to calculate SPI, for rainfall accumulation for a period (for example 1,3, 4, 6, 12 or 48 months, firstly, the two parameters, 'shape and scale' of the gamma distribution are fitted on the frequency distribution for all years in the available time series, and then transform into standard normal distribution to compute SPI. In this study, the seasonal rainfall (JJAS) was fitted in gamma distribution and its distribution function is given as:

$$f(x) = \frac{1}{b^a \Gamma(a)} x^{a-1} e^{\frac{-x}{b}}$$

for x < 0, where a < 0 and b < 0 are the shape and scale parameters, respectively, x < 0 is the rainfall and Γ(a) is the gamma function.

The transformed seasonal rainfall data with zero mean and unit variance of the SPI, helps in computing statistical comparison of wet/flood event (positive SPI) and dry/drought event (negative SPI) across different spatial scale. Based on the threshold value of SPI, flood and drought duration (D) and magnitude of severity (S) has been calculated. The flood and drought duration are the period of the length in which SPI is continuously positive and negative respectively.

Thereafter, the flood and drought can be characterized by its duration, severity and frequency of occurrences. The flood and drought severity are cumulated SPI value within the flood and drought duration, which is defined by:

$$S = -\sum_{i=1}^{D} SPI_i$$

and the intensity of the drought is defined by the ratio of severity of drought to its duration and vice versa for flood. The flood and drought frequency in different categories have been determined (unit; %), these percentage values are expected from a normal distribution of SPI. For example, 2.1% of SPI value within 'ED' category is a percentage that is typically expected for an 'extreme' event. After that, EOF analysis (Lorenz, 1956) has been performed to identify the flood and drought regionalized variability for the period 1981–2015. This method allows for the decomposition of the three-dimensional variable field into orthogonal spatial modes and time series, that have physical meaning and contain specific information about the original field. Mathematically, EOF analysis uses a set of orthogonal functions to represent a time series in the following way:

$$Z(x,y,t) = \sum_{k=1}^{n} PC(t) \bullet EOF(x,y)$$

where, Z(x,y,t) is the original time series as function of time (t) and space (x,y), EOF(x,y) shows the spatial structure (x,y) of the major factors that

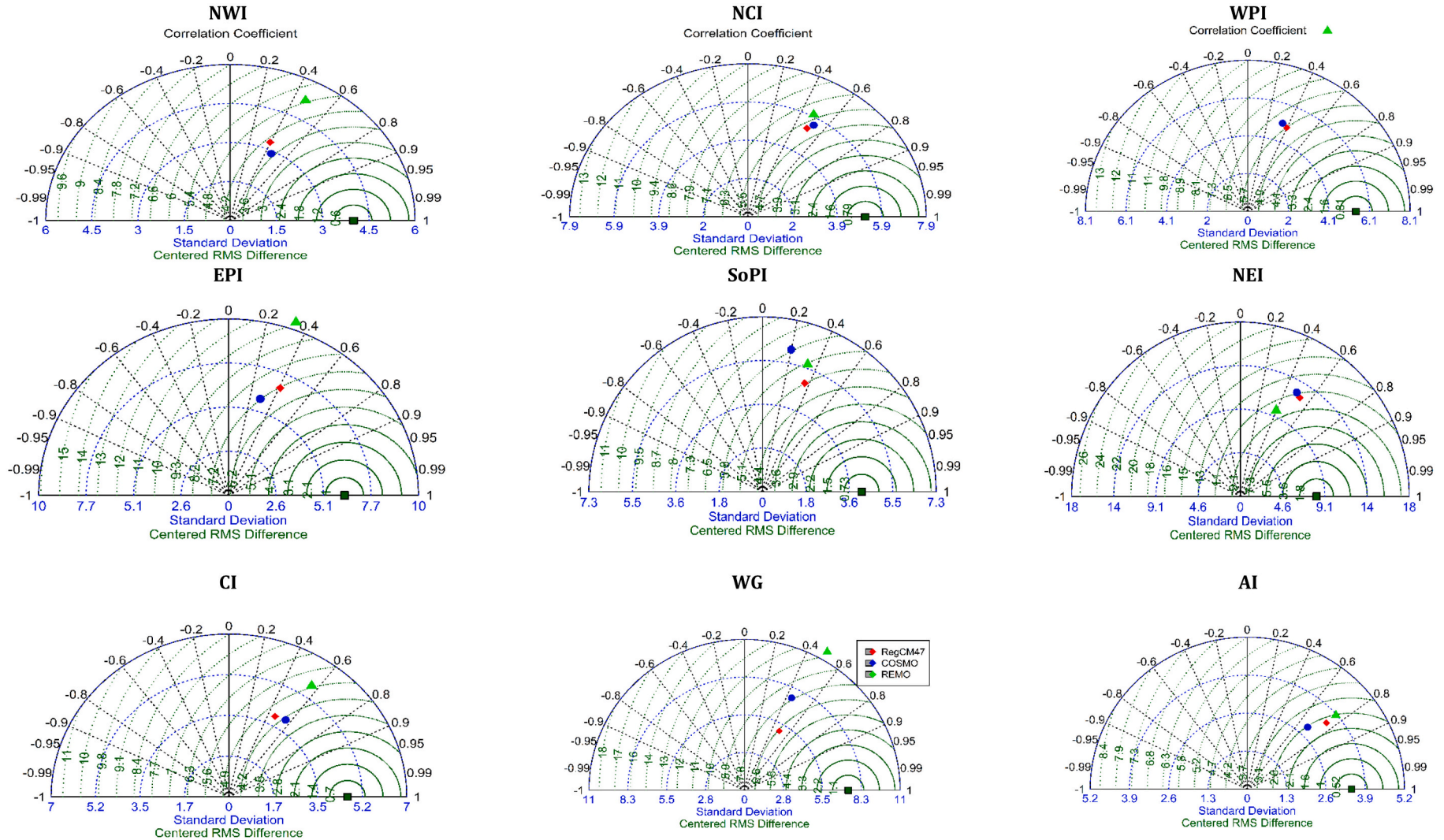

Fig. 2. Taylor diagram for intercomparison of SA-CORDEX RCMs (RegCM4.7, COSMO & REMO2015) and observed data (IMD). *The reference point at a unit distance and 0degree from the origin indicates the perfect performance. The distance to the reference point indicates the normalized root mean square error between the modelled and observations. The radial distance from the origin specifies normalized standard deviations, and cosine of azimuthal positions shows the spatial correlation between the models and observations.

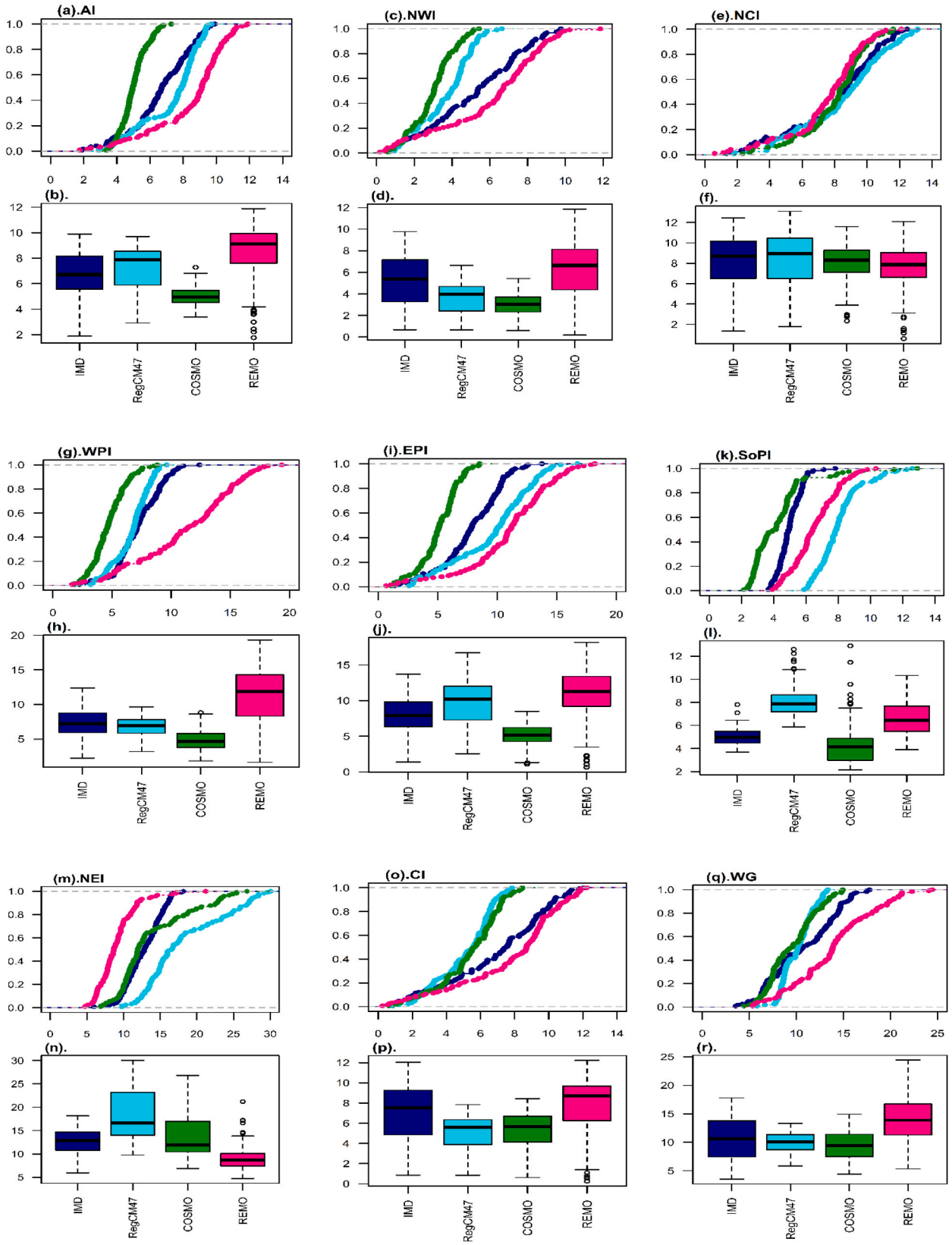

Fig. 3. a-r The empirical cumulative distribution function (ECDF) plot and boxplot of daily ISMR climatology (mm/day) over all India and its subregions during 1981–2015.

account for the temporal variation of Z. The principal component PC(t) signify the amplitude of each EOF varies with the time.

3. Result and discussion

3.1. Model evaluation

The spatial behavior of the observed climatological mean of the Indian summer monsoon rainfall (ISMR) is shown in the Fig. 1(a). The accumulated rainfall pattern shows the lowest rainfall over NWI and SoPI except WG i.e., in the range of 2–4 mm/day. On the other hand, the maximum rainfall is observed in the range of 24–32 mm/day over the mountainous region of WG and NEI. The Indo-Gangetic Plain (IGP) along with the CI experienced moderate rainfall. The observed spatial ISMR distribution compared with the ERA-Interim driven three RCMs simulations (RegCM4.7, COSMO and REMO2015) (Fig. 1b-g). The performance of RegCM4.7 is relatively good in simulating mean ISMR distribution over India and its sub-regions and is capable of simulating areas of minimum and maximum rainfall rates (Fig. 1b) except over the NEI where the simulation shows higher average rainfall (18 mm/day) than the IMD (CI: 12.8 mm/day). Also, the spatial distribution of the mean bias illustrated in the Fig. 1c, which depicts that the RegCM4.7 clearly overestimated (~4–6 mm/day) the mean rainfall along the mountainous topography of WG, WPI, NEI and foothills of the Himalaya (Fig. 1c). This unlikely enhanced rainfall is concerned with the drawbacks of the regional climate models as they overestimate orographic precipitation (Halder et al., 2015; Gao et al., 2015; Gerber et al., 2018).

The previous studies of Singh et al., 2017; Choudhary et al., 2019; Bhatla et al., 2019 reported a large underestimated value of ISMR simulation by RegCM4 over the CI and Gangetic plain of India, however state of art in model shows the remarkable improvement in simulating ISMR in the latest model (RegCM4.7) experiments (CORDEX-CORE) as compared to the previous CORDEX experiments (Shahi et al., 2021). The phenomena of intense precipitation over WG are typical upwind of the topographic divide which sharply decreases magnitude and duration on the leeward side (Barros and Lettenmaier, 1994) clearly shown by the RegCM4.7 simulations. The COSMO simulated rainfall was not distributed as observed in IMD over the Indian subcontinent. According to the IMD rainfall distribution highest rainfall occurs in the west coast, WG, sub-Himalayan areas in the NE, west Bengal and southern slope of eastern Himalayas which is not correctly portrayed in the COSMO simulation, it has been showing high dry bias (~6 mm/day) over highest rainfall regions (Fig. 1d-e). On the other hand, the north and central regions of India including NEI showing normal rainfall in the range of 8–12 mm/day in COSMO RCM. The spatial ISMR simulation over the NEI is best represented by the COSMO as compared to IMD. Next, the precipitation simulation of REMO2015 RCM displayed a satisfactory amount of ISMR over WG, CI and NEI except excess precipitation over the WPI, EPI region (Fig. 1f-g). The previous model version of REMO

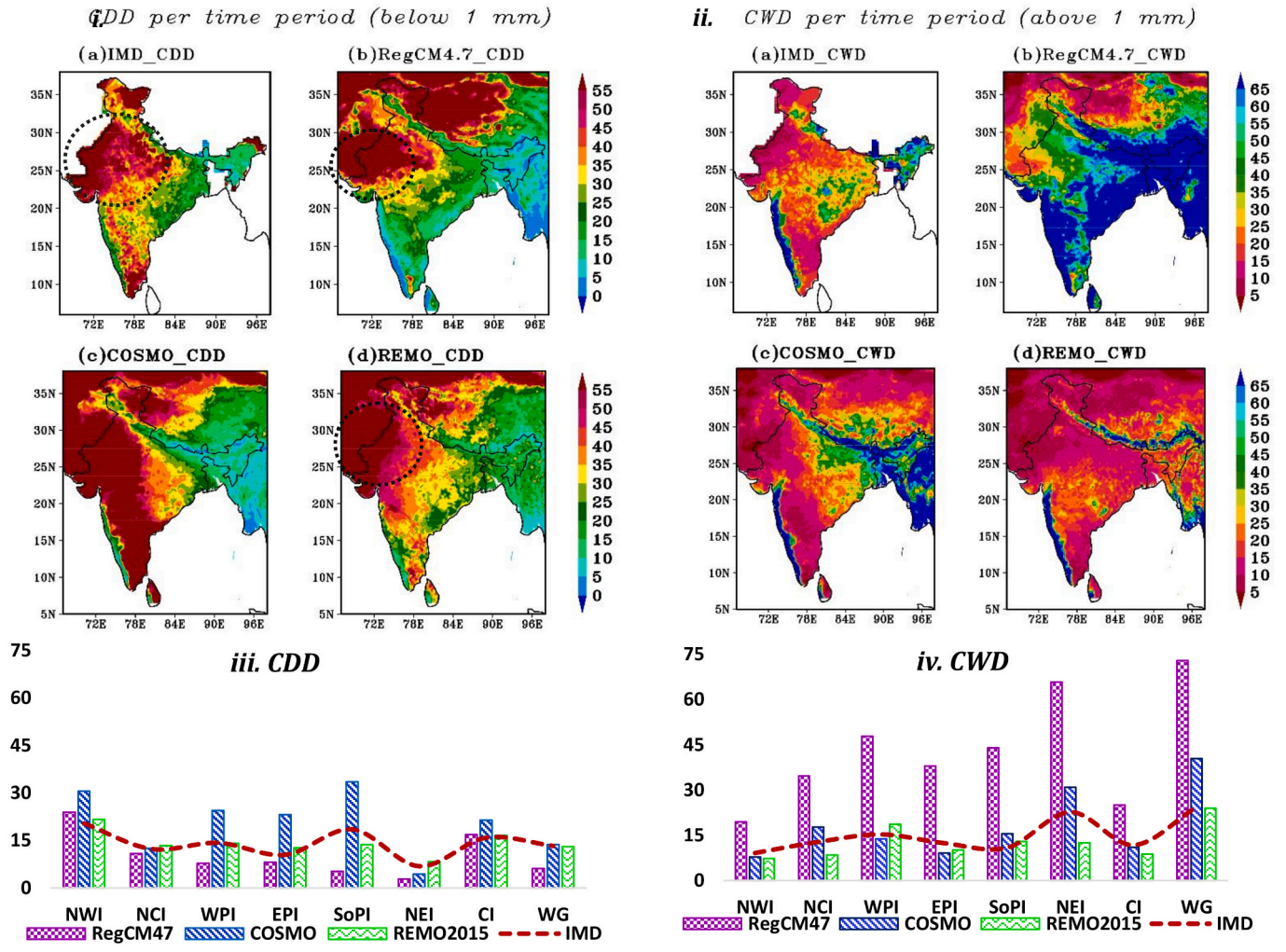

Fig. 4. (i-ii) Climatological spatial temporal distribution of mean consecutive dry days (CDDs) and consecutive wet days (CWDs) observed by (a) IMD and simulated by (b)RegCM47, (c) COSMO and (d) REMO Climate RCM for the period 1981–2015.

Table 4
Observation trend of precipitation indicators over sub regions for 1981–2015.

	MR	*CDD*	*CWD*	*WD*	*HPD*	*VHPD*	*MDI*	*SPI4*
NWI	0.01	0	-0.03	0	0.02	0.02	0.04	0.01
NCI	-0.03*	0.04*	-0.08*	-0.21*	-0.13*	-0.08*	-0.02	-0.04*
WPI	0.01	-0.01	0.02	-0.03	0	-0.01	0.03	0
EPI	0.01	0.01	-0.05	-0.11	-0.05	-0.01	0.04	0.01
SoPI	0	-0.05	0.02	0.04	-0.01	-0.01	-0.02	0
NEI	-0.08*	0.04*	-0.4*	-0.44*	-0.35*	-0.18	-0.02	-0.05*
CI	0	0.01	-0.04	-0.08	-0.02	-0.01	0.02	0
WG	0.02	-0.02	-0.03	0.06	0.06	0.04	0.02	0.01

*Significant at 90% confidence level using Mann Kendall statistics.

mentioned in Jacob et al. (2012) showed remarkable improvement in simulating rainfall over CI in the recent CORDEX REMO2015 (Remedio et al., 2019). The excessive wet bias (~6–8 mm/day) over the EPI region might affect the performance of REMO2015 in simulating the ISMR and its modulated properties over a particular region. The scientific explanation of REMO2015 shows unexpected dry bias all over the Himalayan and northern plain region of India this might be explained with complex orography over the Himalayan region and scarce observational dataset. The distribution of ISMR over the WG, CI and NCI are sensitive for qualitative and quantitative evaluation of RCMs to portray the progression of monsoon.

Descriptive analysis of SA-CORDEX RCMs has been performed with the help of mean bias, SD, RMSE, ECDF and box plot. From Taylor diagram (Fig. 2) it can be concluded that the RCMs (RegCM4.7 & REMO) simulation for daily monsoon precipitation showing significant correlation i.e., 0.8 and least RMSE i.e., ~2.0 mm/day for AI respectively, the SD value of RegCM4.7 (3.3 mm/day) is much closer to the IMD than REMO (3.9 mm/day). On the other hand, COSMO performance was less close to the IMD as compared to the RegCM4.7 and REMO, it was showing 0.65 correlation value with RMSE 2.0 mm/day. In Fig. 3 RCMs intercomparison verified with the support of ECDF plot and box plot over AI. During 35-year climatology of ISMR RegCM4.7 stands very close to the observation (IMD) rainfall (Fig. 3a), on the other hand, COSMO's ECDF underestimated the cumulative rainfall distribution Interquartile distribution with difference of −2 mm/day from IMD. Further, the REMO simulation of ISMR was showing overestimated ECDF and interquartile distribution by +2 mm/day than the IMD distribution. The RCMs simulation is dependent on diversification of the topographical difference of the Indian subcontinent and causes the regionalized difference in simulating monsoon rainfall over its sub-regions (Bhatla et al., 2019), therefore ISMR distribution based on selected sub-regions were considered for further analysis. In the NWI regions, all the RCMs were displaying a high RMSE value which is above 3.6 mm/day from the observational data. CC and SD values were very high for REMO over the NWI region which is justifiable from ECDF and box plot distribution (Fig. 3c&d). Another important sub-region from the northern plain of India is NCI which consist of the fertile region of IGP and RCM performance showing good CC (~0.5), less SD (5.9) except the high value of centered RMS value have been observed from Taylor diagram (Fig. 2). The RCMs precipitation data is equally and well distributed along with the IMD data (Fig. 3e&f). The RCM's ISMR distribution was showing greatly extended dispersion over the western and eastern peninsular India especially in REMO (Figs. 2 & 3g-j). this might be the reason behind the high wet biases (2–8 mm/day) in REMO climatological variation of ISMR. Therefore, only RegCM4.7 closer to the observation for WPI region (Taylor diagram). The COSMO simulated ISMR over WPI and EPI was underestimated as compared to the IMD data (Fig. 3g-j). Taylor diagram for SoPI region elucidates all RCMs showing less CC, high SD & RMSE (above 5.1 mm/day), in which RegCM4.7 was the best performing RCM but ECDF and box plot distribution signify COSMO as best performing among all RCM (Fig. 3k&l). The average observational rainfall over NEI is very high i.e., 13 mm/day (IMD), The undulating terrain and majestic peaks over the NEI provide natural lifting of moisture/rain-bearing cloud from the Bay of Bengal (BoB) and resulted in moderate to very heavy rainfall. Rajeevan et al., 2010 mentioned CI as very crucial and critical region to study the interannual variation of ISMR because it is highly correlated to the all-India monsoon rainfall. Over the CI region, RCMs CC was in the range of 0.5–0.6, COSMO and RegCM4.7 come closer to the observation SD with less RMSE value (~4.2 mm/day) Fig. 2. The ECDF and boxplot interpretation for the CI region depict that RegCM4.7 and COSMO simulated rainfall underestimated from the observed value on the other hand, REMO's rainfall overestimates ISMR observed distribution. After NEI, WG is receiving enough monsoon rainfall during onset i.e., 131 cm, over this region RegCM4.7 and COSMO fits better than REMO scheme (Fig. 2 & 3q&r). The high RMSE value of REMO justifies by the heavy precipitation distribution over the WG region. From the ECDF plot analysis, it has been found that the RCM REMO overestimates the rainfall distribution over peninsular regions on the other hand RegCM4.7 and COSMO performs better in simulating ISMR over most of the sub-regions of India.

3.2. *Spatio-temporal analysis of climate precipitation indices in terms of duration, intensity and frequency*

The CDDs are defined as the maximum number of days with rainfall less than a certain threshold i.e. 1 mm (Frich et al., 2002; Zolina et al., 2013). Previously the spatial and temporal variation and trend of dry and wet periods over India have been studied by Verma and Bhatla, 2021, which indicates increasing CDD over NWI and southern peninsula. On a wider scale, CDDs or dry period variation were analyzed over NWI, NCI, WPI, EPI, SoPI, NEI, CI and WG during monsoon (Fig. 4i(a-d)) during 1981–2015. The spatial maximum observed (IMD) distribution of average CDD (above 45 days) has been widely spread over the NWI region, including Gujarat, upper IGP, eastern Himalaya, Northern NEI and eastern part of SoPI (Fig. 4i(a)). The medium range of CDD (~20–30 CDD) spread over WG EPI and NEI region depicted from the IMD data. The comparative assessment of SA-CORDEX RCMs in simulating CDD presented a clear picture of the length of the dry period which reflects the degree of dryness in the model which eventually provides information about drought variation during the summer monsoon. The length of the dry period primes the factor of drought due to insufficient rain which eventually disturbs agriculture production, vegetation growth and public water supply. The SA CORDEX RCMs simulation of the CDD demonstrated in Fig. 4i(b-d), RegCM4.7 and REMO showed the best spatial representation of CDDs than COSMO. After that, COSMO shows a huge overestimation of about 20 dry days over AI except for WG, NCI and NEI. The temporal average CDDs showed the highest average dry days over NWI i.e., 20 days and lowest over the NEI i.e., 7 days during the monsoon period. From Table 4 significant trend of CDD over different sub-regions has been calculated to examine the variation of dry days during 1981–2015. Most importantly two regions NCI and NEI

Table 5
Classification of flood and drought category based on standardized precipitation index (SPI) (McKee et al., 1993).

Categories	Flood	Drought
Extreme	Above 2.0	−2.0 or less
Severe	1.5 to 1.99	−1.5 to −1.99
Moderate	1.0 to 1.49	−1.0 to −1.49
Near normal	0 to 0.99	0 to −0.99

were showed a significant increasing trend in 35 years. The climatologically increasing trend of dry days are indicating a very serious situation of increasing drought as a result of less precipitation, the reason behind this trend is explained by the drastic and rapid surface warming over India since 2002 (Jin and Wang, 2017) due to land use/land cover change and large-scale circulation change (Paul et al., 2016). The study of Krishnan et al., 2020 described that the effect of anthropogenic aerosol forcing over the northern hemisphere cause decline in the ISMR. The significant decreasing trend of CDDs over SoPI during climatology indicates more intense precipitation events will occur in near future.

The CWD indicates the maximum number of consecutive wet days with a daily rainfall amount at least 1 mm. The observational average spatial distribution of CWD highlighted in Fig. 4ii(a) showed 15–20 CWDs overall India except for high monsoon rainfall regions such as WG (above 60 days), CI (35–40 days) and NEI (55–60 days). The highest value of CWDs over WG, NEI and CI indicates a high chance of flooding. The RegCM4.7 simulations for CWDs was highly overestimated overall in India. Though, the precipitation simulation shows CWDs characteristics very well in COSMO followed by REMO, these RCMs capture the similar pattern of wet spell days as observation (Fig. 4iic&d). During the climatological period, IMD observed the lowest value of CWDs over subregions such as NWI (9), EPI (11), SoPI (11) & CI (12), on the other hand, CWDs values were very high over WG (24) and NEI (23). The average regionalized value of CWDs which are simulated by both RCM COSMO and REMO hold satisfactorily over NWI, WPI, EPI, SoPI, CI as compared to the IMD data. The COSMO simulated CWDs were overestimated over NCI, NEI and WG on the other hand REMO underestimated average CWDs over NCI and NEI.

The NEI region is receiving the maximum amount of rainfall (during the monsoon period but its erratic nature and topographical constraints affect the regional forcing in the RCM thus affecting the values of precipitation counts. Furthermore, the significant decreasing interannual trend has been observed over NEI (−0.4 day/year) and NCI (−0.08 day/year) clearly indicates the weakening of monsoon rainfall over these important regions (Table 4). The NWI India received the least number of wet days with no trend, but HPD and VHPDs trends are slightly increasing in changing climate. This may be explained by monsoonal wind flow which is northwestward from the BoB onto the subcontinent so that most of the moisture is depleted before reaching the NWI region. Among all selected subregions, five regions showed a decline in the wet days (WDs) during 1981–2015, which shows that WDs/number of rainy days (rainfall is 1 mm or more) is decreasing at an average rate of −0.23 days for every decade for all India. A similar decreasing pattern for the interannual WDs has been observed over NEI (−0.44) and NCI (−0.08) and EPI (−0.11) and CI (−0.08). The possible region behind these decreasing rainy days is probably linked with the low cloud cover which is responsible for bulk rainfall during the monsoon period is declining by 0.45%/decade on average (Jaswal et al., 2017). Clouds are the main cause behind the interannual and decadal variability of radiation balance on earth/global energy balance. Thus, low-clouds cause uncertainty in climate model predictions (Solomon et al., 2007). The major erratic behavior of rainfall observed over WGs i.e., decreasing trend of CWDs and increasing trend of WD, HPD, VHPD Table 4. The WG regions received more no. of WDs, HPD (rainy days>20 mm) which is indicated by their increasing trend value i.e., 0.06 in recent times. The value of VHPD (rainy days>25 mm) was slightly increasing over the WG region. Rajeevan et al., 2008 had highlighted the monsoon season may be unaltered over the core monsoon region, however, the extreme precipitation events have shown an increasing trend in the last five decades (Mishra et al., 2012). Thus, recent erratic climatic behavior over the most ecologically rich regions of India i.e., WG clearly observed as no change in mean monsoon climatology but significant increase in the extremes (such as HPD and VHPD), also plays a crucial role in deciding the climatological characteristics of the country. The previous study by Jha et al., 2020 discussed the significant climate warming signal (~ 0.8 ± 0.2 (SD) °C) of the WG of India in the past century. The possible explanation of this behavior is associated with climate warming, which impact our country in terms of loss of biodiversity, heatwaves, droughts and flooding in the coastal regions (Das et al., 2020). The long-term increasing trend of MDI over the NWI, WPI and EPI might be explained by the changing precipitation characteristics under temperature warming (Trenberth et al., 2003; Giorgi et al., 2011).

The annual standardized departure of WDs and MDI conceptualized the whole summer monsoon modulation in rainfall pattern over different sub-regions of India (Fig. 5a-i). Firstly, the NWI region showed the more positive (1983,1994, 2003, 2011 & 2013) and negative (1987, 2002, 2009 & 2015) departure in the case of WDs. Also, frequent and

Table 6
list of monsoonal drought and flood onset year based on SPI4 Index delivered by IMD and SA-CORDEX RCMs (RegCM47, COSMO & REMO2015).

Drought years								
AI	***NWI***	***NCI***	***WPI***	***EPI***	***SoPI***	***NEI***	***CI***	***WG***
1982*#	**1987** *#	2002@	1985	1984	1987#	**1994**	1987#	1985*
1986*	2000	2004*	1986	**1987**	1999	1996	2000	1986
1987	**2002**	**2009***#	1987	1997#@	2001#	**2006***#	**2002@**	**1987**
2002@	**2009***#@	**2010***#@	2015*#@	**2002#**	**2002#@**	2009@	**2009***#	2001#
2004#@		2014 #		2004*#@	**2003*@**	**2011**		2002#
2009*@		**2015** *#		**2009*@**		**2013***#		**2015*#@**
2014*#@								
2015*#@								
Flood years								
AI	***NWI***	***NCI***	***WPI***	***EPI***	***SoPI***	***NEI***	***CI***	***WG***
1983*	1983	1984*	1983*#	1983*#	**1981**	**1987**	**1990*#@**	1983*#
1988 *@	1990 *#	1990*@	**1988*@**	1988*#	**1983*#@**	1988*#	**1994@**	1994#
1990*@	1994@	**1994#**	**2005***	1989*	1988 *#@	1989	2003*@	**2005**
1994	2011#@	1999#@	2006*@	1994	1996*#	1990	**2011@**	2006*#
2005	**2013**	2003#@		**2006**	**2007***	**1993**	**2013**	2007#
2007*#		2008@		2007#	**2011***	**1998*#@**		2011#@
2011#@		2011*@		2010				2013
2013				2013#				

Note-Severe & extreme event highlighted in bold; *RegCM47, #COSMO, @REMO.

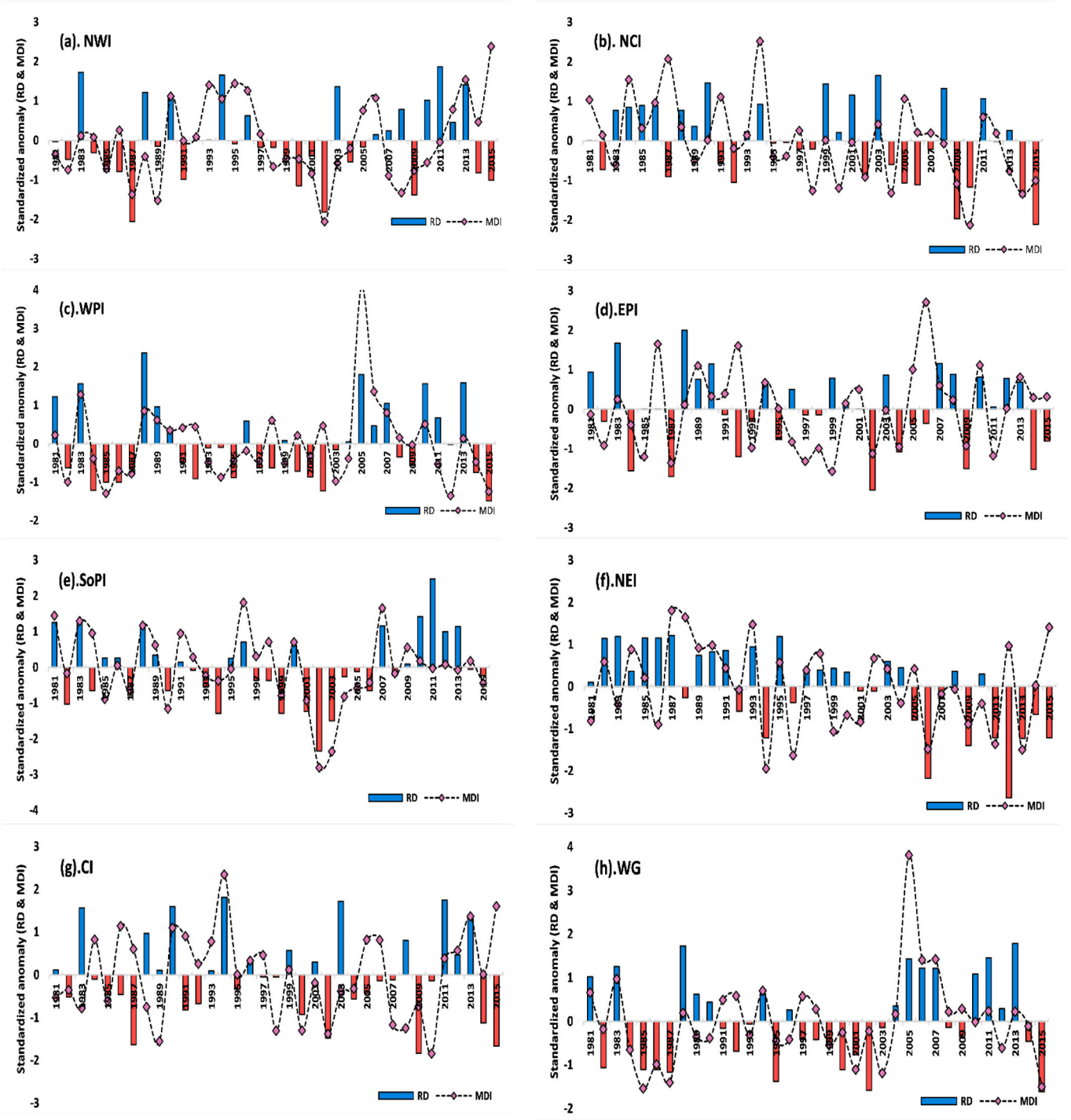

Fig. 5. a-i Standardized observed annual departure of rainy days (RD) and mean daily intensity (MDI) over different subregions during period of 1981–2015.

extreme negative departure in the RDs has been observed after 2002 in the NCI (Fig. 5b). The revival of the monsoon after 2002 shows a significant reduction in WDs which is linked with the large-scale ISM system (Jin and Wang, 2017). This year (2002) was an extremely widespread drought mainly over the northern and western parts of India, as the monsoon failed to advance and cover a large part of NWI and IGP. Due to this 56% of the land experienced low monsoon rainfall, affecting nearly 300 million populations and the loss was phenomenal in every aspect economic, social, livestock etc. The El Nino event in 2014/2015 cause warming over the Indian ocean (Dai et al., 2013) and produces a dry anomaly in 2015 over NCI, NEI, WPI & WG. In Fig. 5c WDs standardized departure shows maximum extent during the 2005 year when WD (+2) and MDI shows +3.5 departure over WPI, this year remarked as Mumbai extremely heavy rainfall (94.4 cm in 24 h), on 26 July 2005 (Chang et al., 2009; Pant et al., 2022). Thus, high number WDs associated with the maximum value of MDI is the indicator for the flood risk in any region. An unusual pattern of high MDI departure has been observed during 2005 and 2006 where number of WDs were very less over EPI region (Fig. 5d). The temporal variability of standardized departure of MDI and WDs over the SoPI region was distinguished by three phases such as 1981–1996(moderate), 1997–2006(dry) and 2007–2013(wet) (Fig. 5e). The NEI regions show a unique temporal

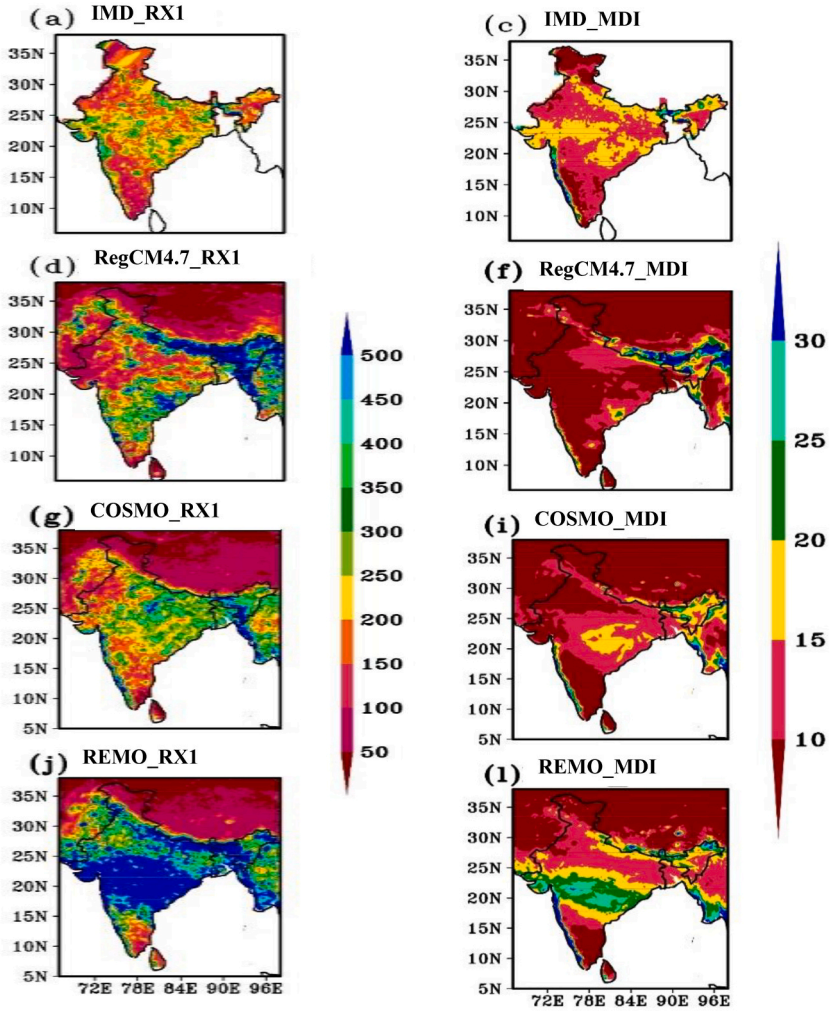

Fig. 6. a-I Climatological distribution of one day highest precipitation (RX1) and mead daily intensity (MDI) over India during 1981–2015.

pattern of which is evidence of decreased no. of WDs and MDIs from 2005 till 2015. In the years 2012 and 2015 MDI value (+2 & +1.5) was showing the highest departure in contradiction with the lowest departure in number of WDs departure i.e., −2.5 and −1. This extraordinary relation of MDI with WD shows that clear evidence of the occurrence of extreme precipitation events in the recent decades (Roxy et al., 2015). Thereafter, most recently high negative departure in WDs observed over CI regions i.e., 2002, 2009, 2014 and 2015, also MDI have been associated with the oscillatory behaviors for example 2015 high MDI associated with least number of WDs indicating weak SWM over the CI but rainfall intensity was high. The WG region received surplus amount of mean ISMR, although the temporal behaviors of WD and MDI indicating a well shifting in the ISMR pattern as after 2004 WD and MDI standard departure was positive as shown in Fig. 5i except 2015. Thus, the temporal pattern of WD and MDI over NEI and WG is alarming and consequently more susceptible to drought and flood events respectively. The report of Pohl et al. (2017) highlighted the fact that the number of WDs and intensity of extreme events cause the major impact on rain-fed agriculture in the tropics.

The spatial distribution seasonal rainfall (JJAS) intensity such as maximum 1-day precipitation amount (RX1; unit-mm) and mean daily intensity (MDI; unit-mm/day) of the observation data and the SA-CORDEX RCMs simulated data (1981–2015) have been describing in Fig. 6a-l. Maximum one-day precipitation is widely distribution along different homogeneous zones of India, in which maximum distribution i.e., above 350 mm of monsoon rainfall found in the region of Gujrat, WG, Meghalaya, CI. The maximum one-day precipitation during monsoon period over NWI and eastern side of the southern peninsula, the upper Himalayan range has been received in the range of 100–200 mm. further, CI and Meghalaya and WG received surplus amount of total one-day precipitation (i.e., ~200–400 mm) in one-day (Fig. 6a) according to the IMD gridded rainfall. The RCM's (RegCM4.7 and COSMO) simulated maximum one-day precipitation is in terms of observation except for the NEI and adjoining zone, where RegCM4.7 overestimate the value (Fig. 6b-c). The IMD data has been showing the MDI value in the range of 15–20 mm/day around the foothills of Himalaya, IGP, upper NEI, WPI, EPI and CI except for some parts of NEI and WG (~20–30 mm/day). The MDI value is very important in case of simulating the characteristics of extreme rainfall over any region. The performance of RCMs RegCM4.7 and COSMO was underestimating the MDI value by 10–15 mm/days especially over IGP and WPI. On the other hand, REMO simulation for one-day maximum precipitation and MDI is overestimated over CI, WPI (25–30 mm/day) and its neighboring region (Fig. 6d&h).

Fig. 7(i)a-d represent the categorically specified precipitation event based on 75th, 90th, 95th and 99th percentile of daily ISMR viz., moderate, wet, very wet and extremely wet rainfall of RegCM4.7, COSMO and REMO with respect to observation data during 35 years (1981–2015). The spatial distribution of IMD's moderate rainfall covering most of India is around 10 mm/days except WG, CI and NEI which is in the range of 20–30 mm/day. In the next category namely, wet rainfall is defined in the range of 40 mm/day for the regions CI and IGP, on the other hand, sub-regions NEI and WG experience different

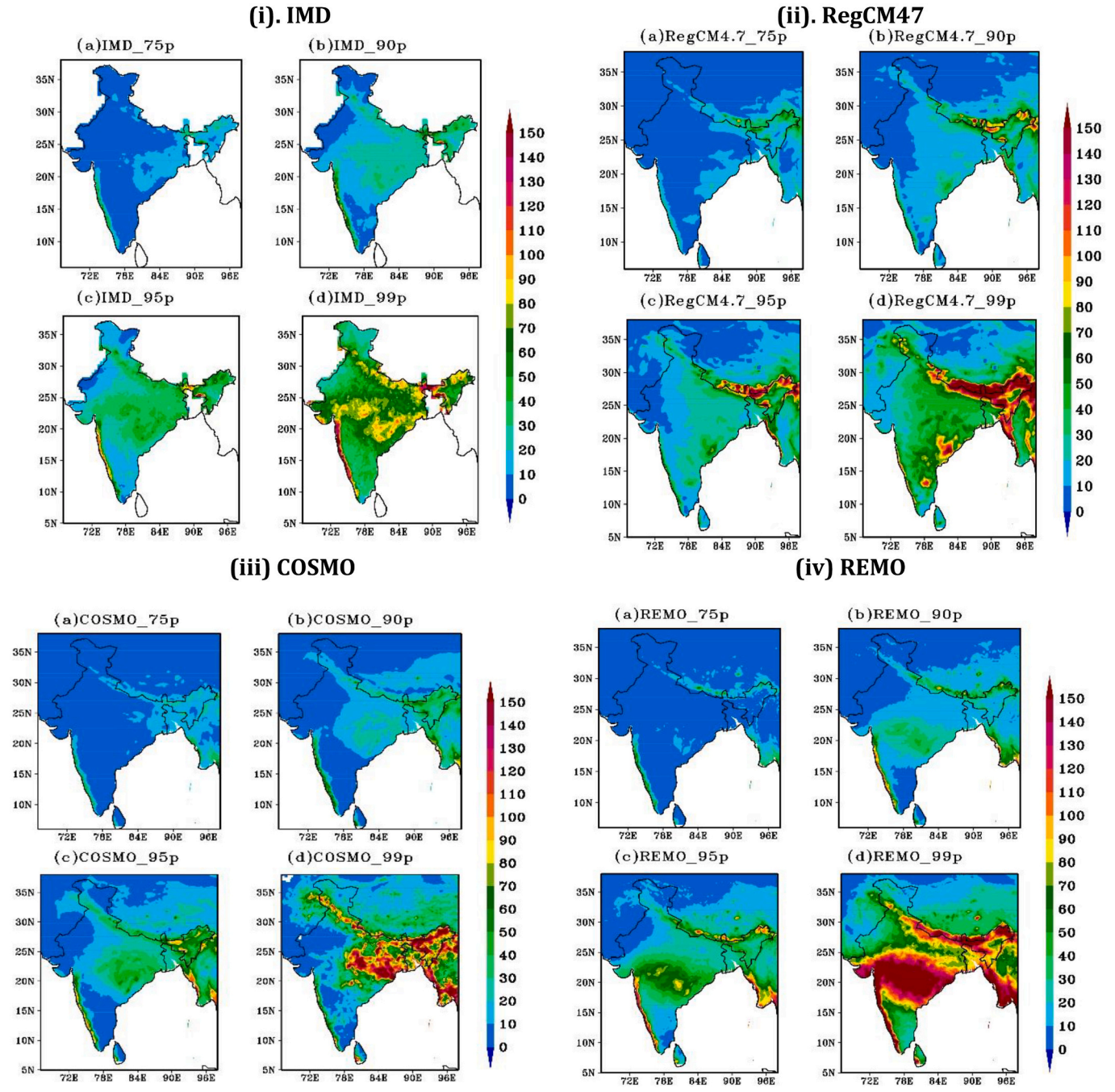

Fig. 7. (i-iv) Spatial representation of categorically specified precipitation event based on 75th,90th,95th, 99th percentile of daily ISMR i.e., moderate, wet, very wet and extremely wet days respectively during 35 years (1981–2010) (i) IMD, (ii) RegCM47, (iii) COSMO and (iv)REMO over India.

thresholds ~50 mm/day. The minimum threshold was achieved by the NWI, the Himalayan and the Eastern part of SoPI (10–30 mm/day) during wet precipitation and very wet precipitation respectively. The scenario of very wet precipitation is accelerated with the regionalized rainfall threshold such as subregion WG and NEI including Sikkim experiencing the elevated threshold of rainfall in the range of 60–90 mm/day, and CI (~50–70 mm/day). Lastly, in the category of extremely wet rainfall days, India's two subregions are worst affected by the extreme rain in the range of 120–150 mm/day viz., WG and Sikkim, the upper part of west Bengal, Meghalaya. Other sub-regions of India, such as CI, EPI, WPI showed the extremely wet rainfall limit in the range of 70–110 mm/day. Also, the regions with low average monsoon rainfall viz., 30–50 mm/day. The RCMs viz. RegCM4.7, COSMO and REMO show the full agreement in simulating the moderate rainfall category similar to the observation. The RegCM4.7 simulations in the category of wet and very wet rainfall is very well distributed but a little bit under-estimated over CI region (Fig. 7ii(a-b)). In the extremely wet rainfall category model simulation has been under-confident when compared with the IMD. In this category, the WG region shows the distribution in the range of 90–120 mm/day which is less in comparison to IMD. Another region of foothills of Himalaya and NEI, RegCM4.7 simulations was highly overestimated (by +50 mm/day) when compared with the IMD (Fig. 7(ii)d), it might be the orography effect of the Himalayan range in the RCM simulation (Sinha et al., 2013). The next RCM COMSO display well simulated the different category rainfall in Fig. 7(iii)a-d. COSMO shadowing rainfall in wet and very wet rainfall category over

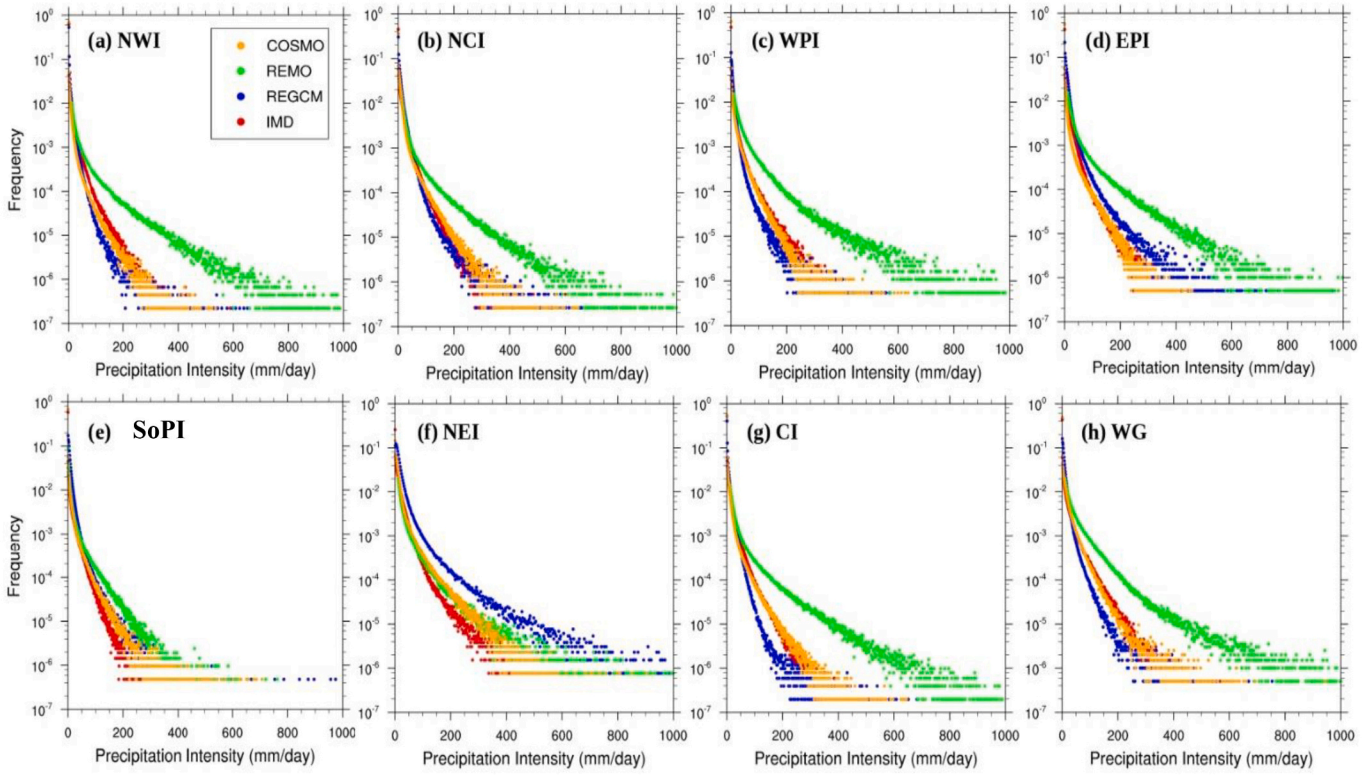

Fig. 8. (a-h) Probability distribution function plot of precipitation intensity over different sub regions of India during 1981–2015.

the eastern side of SoPI and NWI in larger extent (~10 mm/day) compare to the observation (IMD). The extremely wet rainfall category spatial distribution has been well dispersed, slightly overestimated and shifted towards the CI and foothills of Himalaya and NEI, otherwise, except these regions all India considerably receiving less amount of the rainfall as compared with the IMD. Further, the REMO performance in simulating the different categorial rainfall distribution during 1981–2015, has been analyzed and compared with the IMD, rainfall in the category of moderate and wet was well explained with the REMO model and very similar with the IMD in terms of spatial distribution. The 95th and 99th (very wet and extremely wet rainfall) category rainfall distribution were heavily overestimated than IMD data showed more than 150 mm/day over WPI, CI and foothills of Himalaya (Fig. 7iv (d)).

The probability distribution function (PDF) of the precipitation intensity (unit; mm/day) is illustrated in Fig. 8(a-h) as a function of daily precipitation amount. Previously the analysis of different category rainfall representation by the different RCM summarized that the RCMs RegCM4.7 and COSMO are far better to represent the categorized regionalized precipitation but on the other hand, REMO overestimated simulation was not in favor of simulating 95th and 99th category rainfall. Thus, the REMO's PDF of the precipitation intensity tends to overestimate the frequency of intense precipitation (more than 200 mm/day), especially over NWI, NCI, WPI, EPI, CI and WG. The overestimation in simulating precipitation intensity might influence monitoring and detection of the regionalized flood episode. The PDF moderate and extreme rainfall intensity illustrate the good agreement with the IMD observation and RCMs RegCM4.7 and COSMO except for REMO. The RegCM4.7's PDF curve is slightly overestimated over the NEI and EPI as compared with IMD (Fig. 8(a-h)).

3.3. *Spatial-temporal distribution of drought and flood in term of occurrence and severity*

After analyzing the different modulating characteristics of the monsoon rainfall in terms of intensity, duration and frequency, further an important aspect has been highlighted as phase transition (flood and drought episode) during monsoon rainfall. The simulation and prediction of flood and drought episodes by the numerical model is still a challenging task for climate scientists. The main intent of this section is to draw a comprehensive picture of conceivable modulation in flood & drought characteristics using observation data (IMD) and RCMs (RegCM4.7, COSMO and REMO) output. The temporal variation of monsoon season SPI4 clearly indicates the occurrence, duration and intensity of flood and drought episodes during 1981–2015 (Fig. 9d).

The major monsoonal drought episode was 1982, 1983, 1986, 1987, 1992, 2002, 2004, 2009, 2014 and 2015 overall India (Table 6). From the meteorological perspective, these droughts are formed due to persistent large-scale disruption in the global circulation pattern of the atmosphere (Namias et al., 1988). Dai et al. (2013) reported in the review article about substantially increasing global aridity and drought areas mainly due to widespread drying since the 1970s. The previous studies show that the prolonged and large-scale drought is associated with the pacific sea surface temperature (SST) anomalies such as El Nino Southern Oscillation (ENSO) (Dai et al., 2013). They also give the prediction for future climate changes should consider the possibility of increased aridity and widespread drought in coming decades. The study of Jin and Wang, 2017 highlights the revival of the monsoon since 2002 (1.34 mm/day/decade) although the GCM failed to capture observed rainfall revival and corresponding trends and land-ocean temperature gradient. Therefore, the lacunae in current GCMs in simulating revival of the tropical precipitation, ENSO, intraseasonal oscillation and another tropical variability (Lin et al., 2006). The RCM RegCM4.7 well suitable for perceiving the drought episode of 1983, 1986, 2014 and 2015, RCM COSMO also found drought years 1982, 1987, 1995, 2009, 2014 and 2015 and RCM REMO also found the major drought year 1982, 1987, 1995, 2002, 2004, 2009, 2014 and 2015 (Fig. 9d & Table 6) over AI. India has been experienced the onset of 2002 extreme drought in the year 1995 which is extended till 2004. This period (1995–2004) has been witnessed longest deficit in summer monsoon (highlighted in Fig. 9 as prolong dryness) depicted by SPI4 might be linked with the

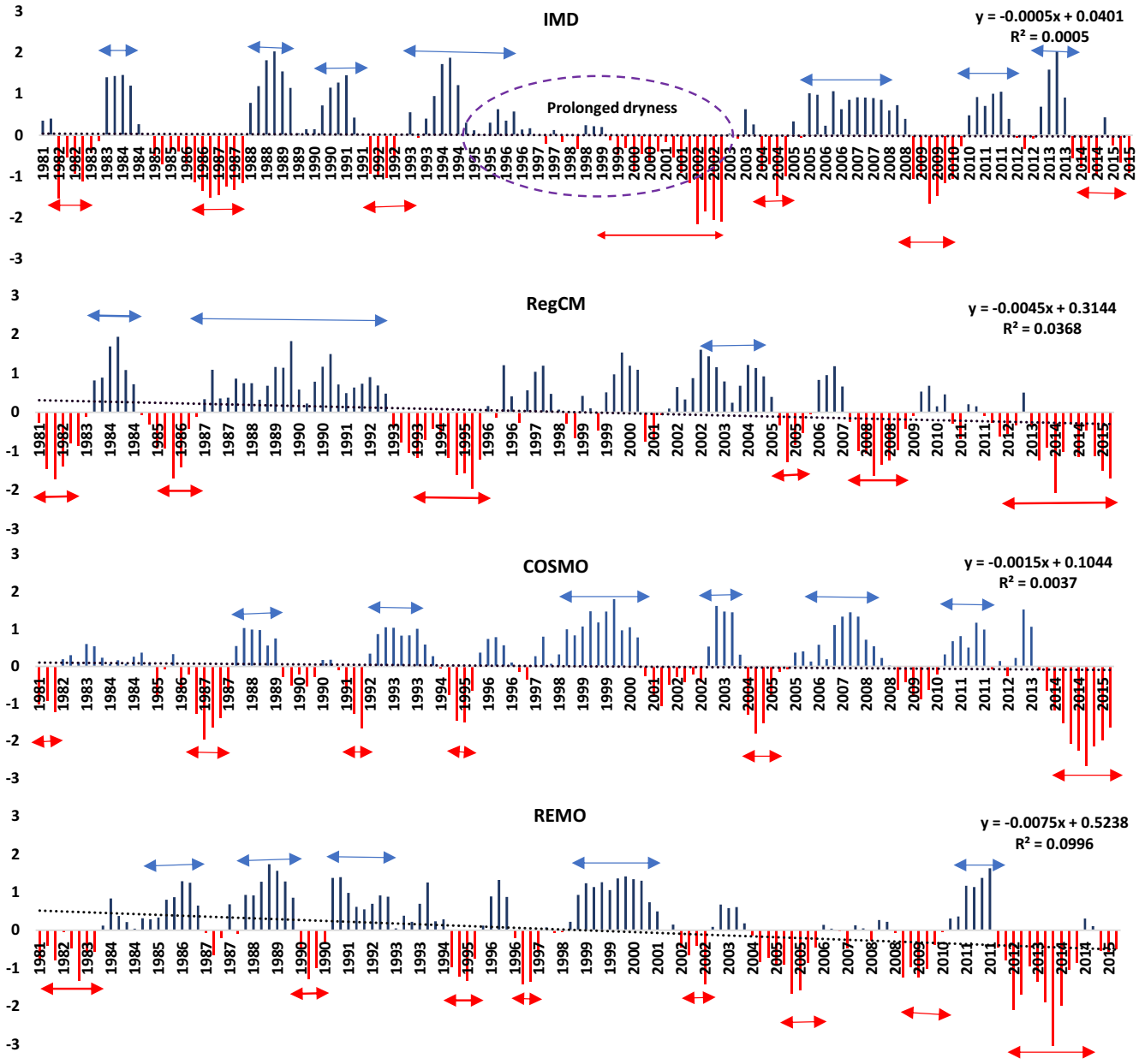

Fig. 9. a-d Temporal distribution of SPI4 value during monsoonal drought and flood observed over All India during 1981–2015 (a). IMD, (b). RegCM47, (c). COSMO & (d). REMO. *Arrow indicating flood duration (◀▶) and drought duration (◀▶).

enhancement of Tropical Indian Ocean (TIO) warming (Zhao and Zhang, 2016) which can be the possible reason behind lack in RCM performance during this period.

The next temporal representation of the drought frequency in different category i.e., moderate drought (MD), severe drought (SD) and extreme drought (ED) has been analyzed with respect to all India and its different regions (in Fig. 10a). All India's MD, SD and ED elucidate as 12.1%, 2.9% and 2.1% respectively extracted from the SPI4 value of the seasonal rainfall. As the model (RegCM4.7) calculated MD (10.7%) frequency has been coming closer to the IMD whereas SD and ED values are in the range 5.7% and 0.7% respectively. COSMO and REMO RCM also, overestimate the SD (5.7% and 6.4% respectively) frequency from the IMD. The more difficult representation of the ED frequency was well captured by the COSMO (2.9%) which is closer to the IMD. The analysis of MD, SD and ED with respect to all subregions and RCMs' performance was complex to explain, thus those subregions showing more frequency of drought category has been explained in this study. Among eight sub-regions highest MD frequency was observed over WPI (12.1%), WG (11.4%), EPI (10.7%), CI (10.7%) and NEI (10.7%) regions according to IMD, and model performance was not consistent to one RCMs. The SD frequency is quite variable among the Indian subregions, in which CI (8.6%) and NWI (7.9%) were severely affected zones as per IMD's SPI4 values (1981–2015). The ED category showed the highest frequency in the SoPI (5%) region, this is probably due to presence of the leeward side of the WG hills which is a drought-prone area because they receive scanty rainfall during the monsoon (Fig. 10(a)).

The temporal distribution of SPI4 values (1981–2015) indicating the flood events i.e., 1983, 1988, 1990, 1994, 2005, 2007, 2011 and 2013 among them 1983 and 1988 AI flood was in extreme flood category (Fig. 9d & Table 6). Recently India did not face any AI flood event in the severe/extreme category because recently flood events are more likely to a localized/regionalized events in term of severity. The emerging

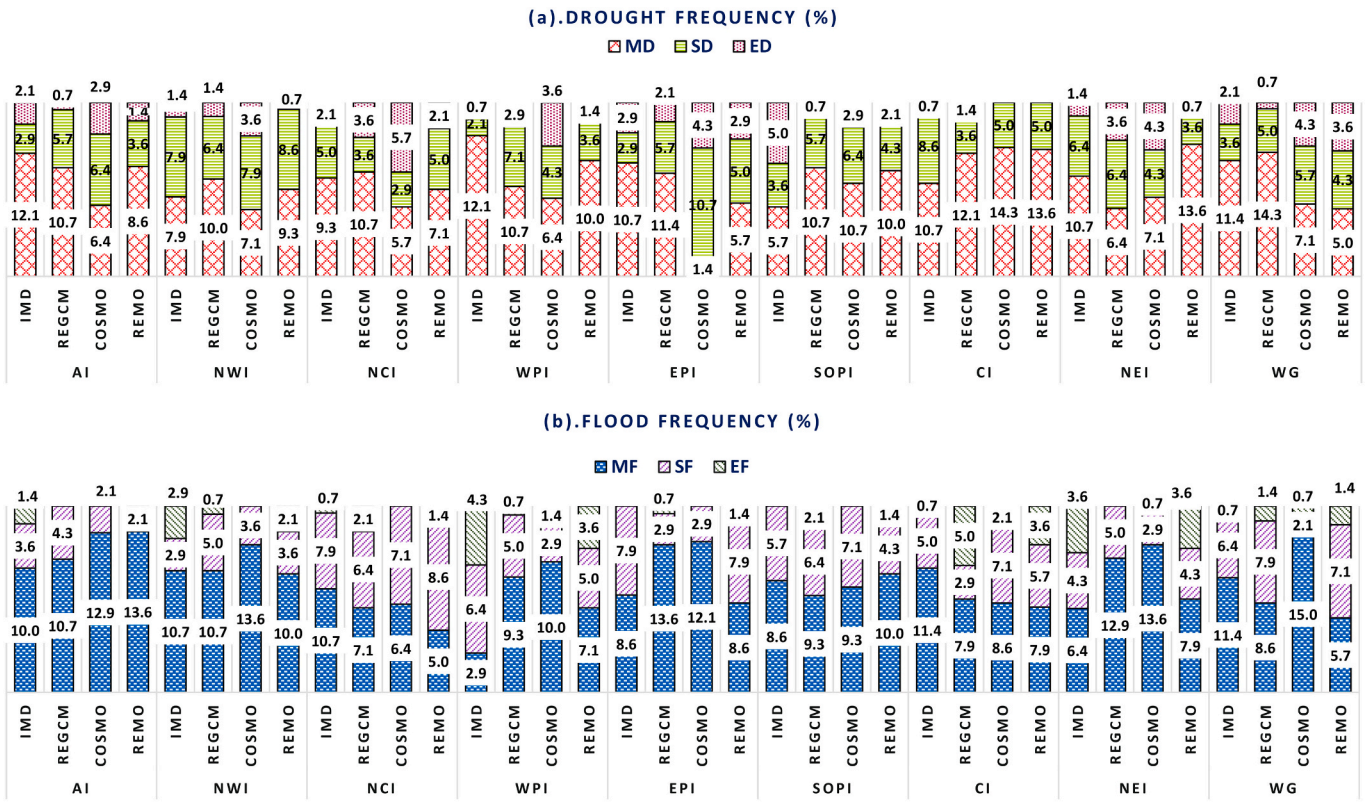

Fig. 10. a-b: The observed (IMD) and RCM simulated flood and drought frequency depicted by SPI4 over AI and its regions during the period of 1981–2015.

hotspot for the major flood affected sub region are NCI, WG and EPI region which experiences almost 7 events (1984, 1990, 1994, 1999, 2003, 2008 & 2011), 7 events (1983, 1994, 2005, 2006, 2007, 2011 & 2013) and 8 events (1983, 1988, 1989, 1994, 2006, 2007, 2010 & 2013) respectively (Fig. 9d & Table 6). The long-range deficient characteristics of nature of ISMR over NEI have not been shown any recent flood case after 1998 which was extreme flood event (major monsoonal flood year over NEI 1987, 1988, 1989, 1990, 1993 & 1998 based on SPI4; Table 6), this may be due to tree cover loss (that's means total canopy lost) in the North east 76% or ~ 1.4 million hectares (Nagaland contribution was maximum), the probable influence of changing local climatic factors and anthropogenic activities such as change in land use land cover (LULC) (Roy et al., 2015; Kuttippurath et al., 2021). The CI region have experienced four major monsoonal flood events such as 1990, 1994, 2011 and 2013 is subject of concern in the recent year. The SA-CORDEXsimulation was well expressed the monsoonal flood in term of duration, and intensity especially in RegCM4.7 and REMO for AI (Fig. 9b-d).

Similarly, in Fig. 9(b) monsoonal flood frequency has been calculated in different category i.e., moderate flood (MD), severe flood (SF) and extreme flood (EF) during 1981–2015 based on SPI4 values. The MF (10%) and SF (3.6%) have been observed over AI which is well represented by the mainly RegCM4.7 simulations, but EF (1.4%) failed to simulate by any of the RCMs. The major contributed MF has been well distributed over all subregions of the India except WPI where SF (6.4%) and EF (4.3%) has largest contribution among flood category. One more region is highlighted in Fig. 10b i.e., NEI which is among the highest rainfall receiving zones of the India observing 3.6% of EF in this region. The model simulation more or less well fitted in calculating the MF and SF over AI, NWI, NCI, SoPI, CI whereas WPI, EPI, NEI and WG were showing large fluctuation in computing flood frequency. Overall, addressing and anticipating modulated behaviors of ISMR in the present climate scenario is critically important for regional adaptation against drought and flood severity at the regional level.

3.3.1. Spatio-temporal pattern of year-to-year variability in drought and flood events using EOF

Drought and flood could be driven by the major characteristics of meteorological and hydrological processes and it is assumed that this structure could be separated into orthogonal sub-climate regimes via empirical orthogonal function (EOF) which can also be referred to as principal component analysis (PCA; Tatli and Türkeş, 2011). This analysis was proposed by Lorenz (1956) in the atmospheric sciences. Here we have applied EOF analysis on the spatial monsoon SPI to reveal the dominant spatio-temporal patterns of regional drought and flood (Fig. 11a–e). The first EOF mode (denoted as EOF1) of the IMD, which explains about 17% of the total SPI variability on the interannual time scale, shows SPI rainfall pattern with anomalous large positive values concentrated over the western peninsular region and extending towards central India as well as the NWI region of India (Fig. 11(a1)). On the other hand, we observed anomalous negative values over the NEI and eastern parts of the Indo-Gangetic Plain. This finding validates with the study of (Mallya et al., 2016) which explains the drought characteristics in terms of duration, intensity, and frequency indicating that droughts are no longer large-scale phenomena, it is converting into regionalized droughts signal over eastern India and IGP. The observed second EOF mode (EOF2) as shown in Fig. 11(a2) is characterized by negative SPI anomalies over monsoon core zone (including the WG) and parts of the western Himalayas and strong positive anomalies over the SoPI and also positive value in the parts of the Indo-Gangetic Plain. The comparison of the EOF1 pattern calculated by the RCMs presented a clear picture of the validation of model output in simulating the drought flood variability on spatial and temporal skill elucidate that RegCM4.7 and COSMO have a similar pattern as IMD and showing the total variance of about 31% and 21% respectively (Fig. 11(b1&d1). On the other hand, REMO is able to show the closest variance (i.e. 15%; Fig. 11(c1)) but it is not able to capture the positive anomaly signature over the WPI and NWI region. The spatial pattern of EOF2 with 11% of total variance obtained from RegCM4.7 shows closest resemblance with the observation and

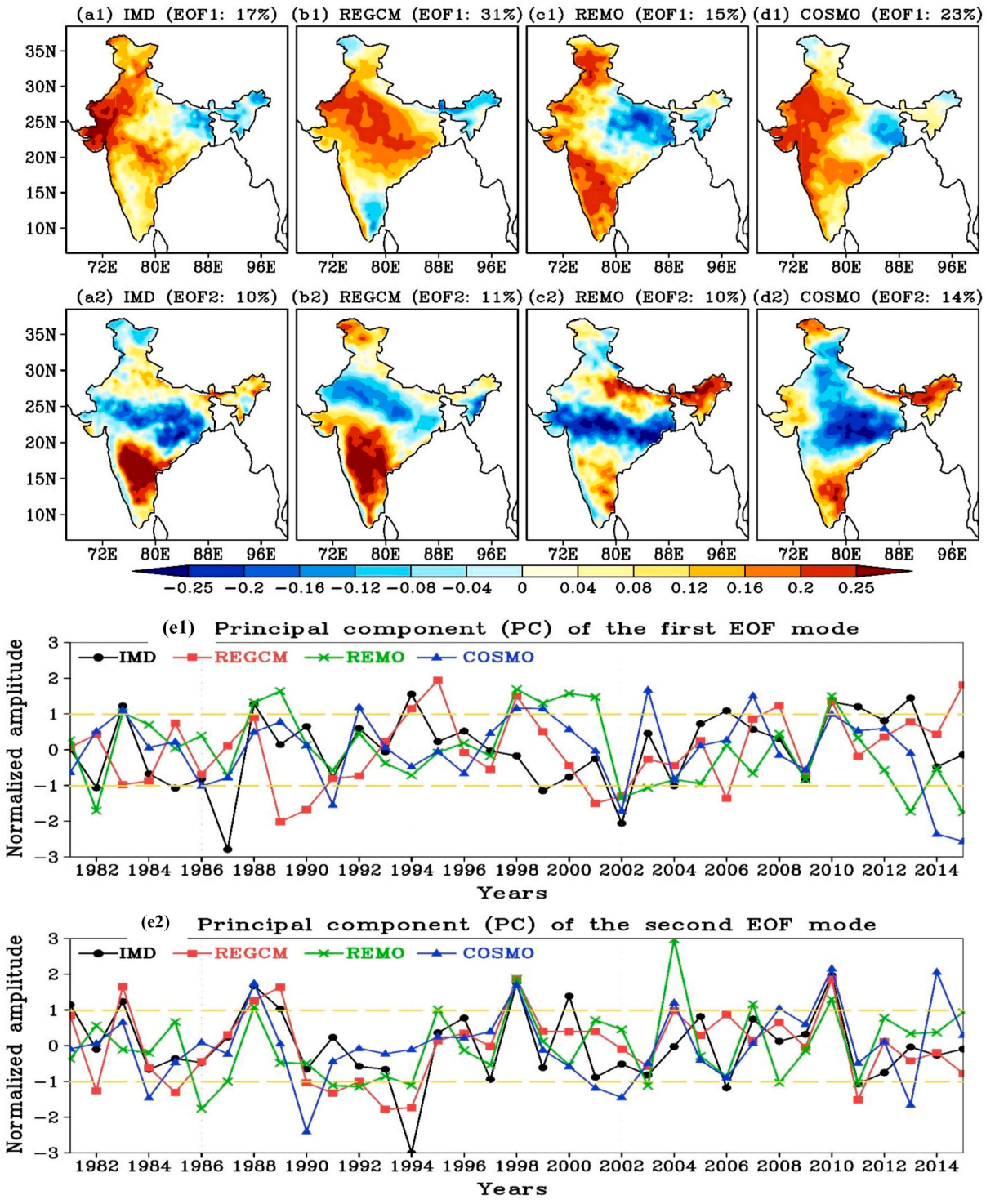

Fig. 11. a-e: The first and second leading mode of EOF of the standardized precipitation Index (SPI) in (a1 & a2) observation (IMD) and CORDEX-SA RCMs'; (b1&b2) REGCM, (c1&c2) REMO and (d1&d2) COSMO; (e1 & e2) indicating temporal distribution of normalized principal component of first and second EOF respectively during 1981–2015. *The percentage of total varaiance explained by each EOF modes is shown in () at the top of each panel.

successfully captures the bipolar distribution of variability over India (Fig. 11(b2-d2)). The corresponding normalized principal component (PC1 & PC2) of IMD and RCMs were used to understand the temporal structure in the prominent modes of variability of floods and droughts (Fig. 11(e1)), the main contributing PC1 explained about the 75% of the flood events (1983, 1988, 1994, 2005, 2011, 2013) and drought event (1982, 1987, 2002, 2004 and 2009) by 62.5% calculated by SPI (Table 6) hence the majority flood and drought event captured by the PC1 proves EOF1 will provides the best possible regional variability of these events in term of severity and occurrence.

The spatial patterns of major drought and flood years are depicted using composite plots. The monsoonal droughts (1982, 1987, 2002, 2004 & 2009) and floods (1983, 1988, 1994, 2011 & 2013) years have been considered for plotting the composite of spatial monsoon SPI of the IMD and SA-CORDEX RCMs (Fig. 12a-h) and most of the events/years coincide with PC1 and PC2. The prominent drought pattern during 35-

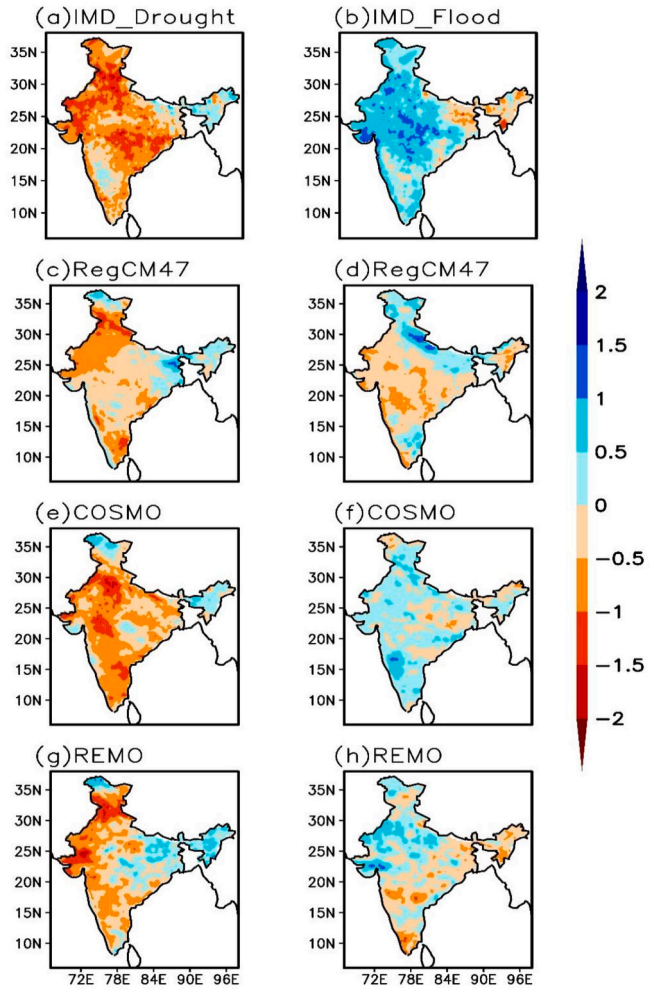

Fig. 12. a-h Composite plot of droughts (1982, 1987, 2002, 2004 & 2009) and floods (1983, 1988, 1994, 2011 & 2013) based on SPI Index (JJAS) (a&b) IMD; (c-d) RegCM47; (e-f) COSMO and (g-h) REMO during 1981–2015.

year climatology covers 80% of India, except lower IGP and NEI, the maximum concentration of drought observed over NWI extending over CI (Fig. 12a). The model performance in capturing the composite of droughts was specially observed in COSMO followed by REMO (Fig. 12e&g). The Intensity of the drought SPI was lower than observation in RegCM4.7 (Fig. 12c). The spatial distribution of SPI flood events in IMD also consists of all India except, Lower IGP & NEI, which highlights that both regions (lower IGP and NEI) acquired different or opposite dynamics from all India to explain the occurrence of flood and droughts (Fig. 12a&b). However, the RCMs performance elucidate the performance of COSMO was best in simulating the flood events over India (Fig. 12f), Instead, RegCM4.7 (Fig. 12d) showed the dryness particularly, over the NWI, CI and WG. The REMO calculate SPI indices showed the dryness/drought pattern over the EPI, NEI and SoPI region (Fig. 12h). Therefore, this study underscores the importance to understand regional variation/variability of the precipitation indices, drought and flood characteristics in the context of futuristic role of models to identify regional hotspots.

4. Conclusions

The Indian summer monsoon is showing phase alteration with frequent moderate to severe drought and flood episodes and the simulation of these episodes is still a challenging task for the climate modeling communities. The WCRP CORDEX community is making efforts to improve the Indian summer monsoon simulation under SA-CORDEX programme. The latest ERA-Interim driven high-resolution RCMs (RegCM4.7, COSMO & REMO2015) simulation has been examined to understand the capabilities of the models in simulating spatio-temporal variation of the mean precipitation (including the wet and dry spells), high impact precipitation events and the drought and floods conditions for the period of the 1981–2015. The significant decreasing ISMR trend dominated over north central India (NCI; −0.03 mm/day) and north east India (NEI; −0.08 mm/day) which are accompanied with significant decreasing trend of consecutive wet days i.e., NEI (−0.4 day/year) and NCI (−0.08 day/year) clearly indicates the weakening of monsoon rainfall over these important regions. Also, the increasing trend of consecutive dry days over these sub regions are indicating a very serious situation of increasing drought as a result of less precipitation, the drastic and rapid surface warming over India since 2002 (Jin and Wang, 2017), land use/land cover change and large-scale circulation change (Paul et al., 2016).

The RCMs has good potential to elucidate the modulation in the ISMR in terms of frequency, duration and Intensity. On the regional scale viz NEI and NCI, significantly increasing drought characteristics (duration, intensity and frequency) had been observed which could be a slow-driver in terms of decrease in mean monsoon rainfall and could also leads to 'critically regionalized hotspot susceptible to drought'. In terms of flood conditions, two critical zones are highlighted as SoPI including the WG region, which can be demarcated in the category of 'critical regionalized flood zones'. The phase modulation synchronization of COSMO simulation during drought and flood were best followed by RegCM4.7 and REMO. The first mode of the EOF exhibits (17% variance) well defined regionalized signature of maximum drought variability over the NCI & NEI region and high floods variability concentrated over NWI, lower CI and WG. On the other hand, the second mode mainly articulated the dipolar structural variation in the flood events (SoPI region except for WG) and drought events (CI region). The main contributing principal component (PC1) explained about the 75% of the flood events (1983, 1988, 1994, 2005, 2011, 2013) and drought event (1982, 1987, 2002, 2004 and 2009) by 62.5%, hence the majority flood and drought event captured by the PC1 proves EOF1 will provides the best possible regional variability of these events in term of severity and occurrence. Inclusively, the latest SA-CORDEX models show considerable skill in simulating various characteristics of the Indian summer monsoon compared to the previous low-resolution SA-CORDEX simulations (~50 km) with same models, which indicates that increasing the resolution of the model can improve the simulation but these models are more susceptible to simulate drought than the flood characteristics in terms of duration, frequency and severity. Interesting and application-based results are obtained that allowed the future application of the methodology in different sub regions of India, in a comparative way to bring out regionalized modulation in the precipitation.

Author contribution

SV, RB developed and designed the research. SV and NKS further developed the research and data analysis. SVs wrote the manuscript which was subsequently modified and supervised by RB and RKM.

Declaration of Competing Interest

The authors declare that they have no known competing financial interests or personal relationships that could have appeared to influence the work reported in this paper.

Acknowledgement

Authors would like to thanks the modeling group for computing and providing the RCM simulations in the frame of the Coordinated Regional

Downscaling Experiment (CORDEX) Framework and COmmon Regional Experiment (CORE). Special thanks to University Grants Commission (UGC) for Senior Research Fellowship (SRF) and Institute of Eminence (IoE) grant, for completion of this study. Thanks to the India Meteorology Department (IMD) for providing the necessary gridded rainfall datasets.

References

Allan, R.P., Soden, B.J., 2008. Atmospheric warming and the amplification of precipitation extremes. Science 321 (5895), 1481–1484.
Asharaf, S., Ahrens, B., 2015. Indian summer monsoon rainfall processes in climate change scenarios. J. Clim. 28 (13), 5414–5429.
Ashfaq, M., Cavazos, T., Reboita, M.S., Torres-Alavez, J.A., Im, E.S., Olusegun, C.F., Alves, L., Key, K., Adeniyi, M.O., Tall, M., Sylla, M.B., 2021. Robust late twenty-first century shift in the regional monsoons in RegCM-CORDEX simulations. Clim. Dyn. 57 (5), 1463–1488.
Baldauf, M., Seifert, A., Förstner, J., Majewski, D., Raschendorfer, M., Reinhardt, T., 2011. Operational convective-scale numerical weather prediction with the COSMO model: description and sensitivities. Mon. Weather Rev. 139 (12), 3887–3905.
Barros, A.P., Lettenmaier, D.P., 1994. Dynamic modeling of orographically induced precipitation. Rev. Geophys. 32 (3), 265–284.
Bhatla, R., Ghosh, S., Verma, S., Mall, R.K., Gharde, G.R., 2019. Variability of monsoon over homogeneous regions of India using regional climate model and impact on crop production. Agribiol. Res. 8 (3), 331–346.
Bindoff, N.L., Stott, P.A., AchutaRao, K.M., Allen, M.R., Gillett, N., Gutzler, D., Hansingo, K., Hegerl, G., Hu, Y., Jain, S., Mokhov, I.I., 2013. Detection and Attribution of Climate Change: From Global to Regional.
Chang, H.I., Kumar, A., Niyogi, D., Mohanty, U.C., Chen, F., Dudhia, J., 2009. The role of land surface processes on the mesoscale simulation of the July 26, 2005 heavy rain event over Mumbai, India. Glob. Planet. Chang. 67 (1–2), 87–103.
Choudhary, A., Dimri, A.P., Paeth, H., 2019. Added value of CORDEX-SA experiments in simulating summer monsoon precipitation over India. Int. J. Climatol. 39 (4), 2156–2172.
Christian, J.I., Basara, J.B., Hunt, E.D., Otkin, J.A., Furtado, J.C., Mishra, V., Xiao, X., Randall, R.M., 2021. Global distribution, trends, and drivers of flash drought occurrence. Nat. Commun. 12 (1), 1–11.
Dai, A., Li, H., Sun, Y., Hong, L.C., Chou, C., Zhou, T., 2013. The relative roles of upper and lower tropospheric thermal contrasts and tropical influences in driving Asian summer monsoons. J. Geophys. Res. Atmos. 118 (13), 7024–7045.
Das, J., Jha, S., Goyal, M.K., 2020. Non-stationary and copula-based approach to assess the drought characteristics encompassing climate indices over the Himalayan states in India. J. Hydrodyn. 580, 124356.
Dash, S., Pattnayak, K., Panda, S., Vaddi, D., Mamgain, A., 2015. Impact of domain size on the simulation of Indian summer monsoon in RegCM4 using mixed convection scheme and driven by HadGEM2. Clim. Dyn. 44, 961–975.
Dee, D.P., et al., 2011. The ERA-Interim reanalysis: configuration and performance of the data assimilation system. Q. J. R. Meteorol. Soc. 137(656), 553–597.
Dhar, O.N., Nandargi, S., 2003. Hydrometeorological aspects of floods in India. Nat. Hazards 28, 1–33.
Frich, P.A.L.V., Alexander, L.V., Della-Marta, P.M., Gleason, B., Haylock, M., Tank, A.K., Peterson, T., 2002. Observed coherent changes in climatic extremes during the second half of the twentieth century. Clim. Res. 19 (3), 193–212.
Gao, Y., Xu, J., Chen, D., 2015. Evaluation of WRF mesoscale climate simulations over the Tibetan Plateau during 1979–2011. J. Clim. 28 (7), 2823–2841.
Gerber, F., Besic, N., Sharma, V., Mott, R., Daniels, M., Gabella, M., Berne, A., Germann, U., Lehning, M., 2018. Spatial variability in snow precipitation and accumulation in COSMO–WRF simulations and radar estimations over complex terrain. Cryosphere 12 (10), 3137–3160.
Giorgi, F., Gutowski Jr., W.J., 2015. Regional dynamical downscaling and the CORDEX initiative. Annu. Rev. Environ. Resour. 40, 467–490.
Giorgi, F., Jones, C., Asrar, G.R., 2009. Addressing climate information needs at the regional level: the CORDEX framework. World Meteorol. Org. (WMO) Bull. 58, 175.
Giorgi, F., Im, E.S., Coppola, E., Diffenbaugh, N.S., Gao, X.J., Mariotti, L., Shi, Y., 2011. Higher hydroclimatic intensity with global warming. J. Clim. 24 (20), 5309–5324.
Giorgi, F., Coppola, E., Solmon, F., Mariotti, L., Sylla, M., Bi, X., Elguindi, N., Diro, G., Nair, V., Giuliani, G., 2012. RegCM4: model description and preliminary tests over multiple CORDEX domains. Clim. Res. 52, 7–29.
Guhathakurta, P., Sreejith, O.P., Menon, P.A., 2011. Impact of climate change on extreme rainfall events and flood risk in India. J. Earth Syst. Sci. 120 (3), 359–373.
Gutowski Jr., W.J., Giorgi, F., Timbal, B., Frigon, A., Jacob, D., Kang, H.S., Raghavan, K., Lee, B., Lennard, C., Nikulin, G., O'Rourke, E., 2016. WCRP coordinated regional downscaling experiment (CORDEX): a diagnostic MIP for CMIP6. Geosci. Model Dev. 9 (11), 4087–4095.
Halder, S., Dirmeyer, P.A., Saha, S.K., 2015. Sensitivity of the mean and variability of Indian summer monsoon to land surface schemes in RegCM4: Understanding coupled land-atmosphere feedbacks. J. Geophys. Res. Atmos. 120 (18), 9437–9458.
Holtslag, A.A.M., De Bruijn, E.I.F., Pan, H., 1990. A high resolution air mass transformation model for short-range weather forecasting. Mon. Wea. Rev. 118(8), 1561–1575.
Jacob, D., Elizalde, A., Haensler, A., Hagemann, S., Kumar, P., Podzun, R., Rechid, D., Remedio, A.R., Saeed, F., Sieck, K., Teichmann, C., 2012. Assessing the transferability of the regional climate model REMO to different coordinated regional climate downscaling experiment (CORDEX) regions. Atmosphere 3 (1), 181–199.
Jaswal, A.K., Kore, P.A., Singh, V., 2017. Variability and trends in low cloud cover over India during 1961-2010. Mausam 68 (2), 235–252.
Jena, P., Azad, S., 2021. Observed and projected changes in extreme drought and flood-prone regions over India under CMIP5 RCP8. 5 using a new vulnerability index. Clim. Dyn. 1-19.
Jha, S., Bharti, B., Reddy, D.V., Shahdeo, P., Das, J., 2020. Assessment of climate warming in the Western Ghats of India in the past century using geothermal records. Theor. Appl. Climatol. 142 (1), 453–465.
Jin, Q., Wang, C., 2017. A revival of Indian summer monsoon rainfall since 2002. Nat. Clim. Chang. 7 (8), 587–594.
Karl, T.R., Nicholls, N., Ghazi, A., 1999. Clivar/GCOS/WMO workshop on indices and indicators for climate extremes workshop summary. In: Weather and Climate Extremes. Springer, Dordrecht, pp. 3–7.
Kodra, E., Ghosh, S., Ganguly, A.R., 2012. Evaluation of global climate models for Indian monsoon climatology. Environ. Res. Lett. 7 (1), 014012.
Krishnan, R., Sanjay, J., Gnanaseelan, C., Mujumdar, M., Kulkarni, A., Chakraborty, S., 2020. Assessment of climate change over the Indian region: A report of the ministry of earth sciences (MOES). In: Government of India. Springer Nature, p. 226.
Kuttippurath, J., Murasingh, S., Stott, P.A., Sarojini, B.B., Jha, M.K., Kumar, P., Nair, P.J., Varikoden, H., Raj, S., Francis, P.A., Pandey, P.C., 2021. Observed rainfall changes in the past century (1901–2019) over the wettest place on Earth. Environ. Res. Lett. 16 (2), 024018.
Lavanya, A.K., 2021. Urban flood management–a case study of Chennai city. Arch. Dermatol. Res. 2 (6), 115–121.
Lin, J.L., Kiladis, G.N., Mapes, B.E., Weickmann, K.M., Sperber, K.R., Lin, W., Wheeler, M.C., Schubert, S.D., Del Genio, A., Donner, L.J., Emori, S., 2006. Tropical intraseasonal variability in 14 IPCC AR4 climate models. Part I: Convective signals. J. Clim. 19 (12), 2665–2690.
Lohmann, U., Roeckner, E., 1996. Design and performance of a new cloud microphysics scheme developed for the ECHAM general circulation model. Clim. Dyn. 12(8), 557–572.
Lorenz, E.N., 1956. Empirical Orthogonal Functions and Statistical Weather Prediction.
Louis, J.F., 1979. A parametric model of vertical eddy fluxes in the atmosphere. Bound.-Layer Meteorl. 17, 187–202.
Luo, M., Liu, T., Meng, F., Duan, Y., Frankl, A., Bao, A., De Maeyer, P., 2018. Comparing bias correction methods used in downscaling precipitation and temperature from regional climate models: a case study from the Kaidu River Basin in Western China. Water 10 (8), 1046.
Mallya, G., Mishra, V., Niyogi, D., Tripathi, S., Govindaraju, R.S., 2016. Trends and variability of droughts over the Indian monsoon region. Weather. Clim. Extremes 12, 43–68.
McKee, T.B., Doesken, N.J., Kleist, J., 1993. The relationship of drought frequency and duration to time scales. In Proceedings of the. In: 8th Conference on Applied Climatology, 17 (22), pp. 179–183.
Meehl, G.A., Arblaster, J.M., Tebaldi, C., 2005. Understanding future patterns of increased precipitation intensity in climate model simulations. Geophys. Res. Lett. 32 (18).
Mishra, A.K., Dwivedi, S., 2019. Assessment of convective parametrization schemes over the Indian subcontinent using a regional climate model. Theor. Appl. Climatol. 137 (3), 1747–1764.
Mishra, V., Dominguez, F., Lettenmaier, D.P., 2012. Urban precipitation extremes: how reliable are regional climate models? Geophys. Res. Lett. 39 (3).
Mishra, A.K., Dwivedi, S., Das, S., 2020a. Role of Arabian Sea warming on the Indian summer monsoon rainfall in a regional climate model. Int. J. Climatol. 40 (4), 2226–2238.
Mishra, V., Thirumalai, K., Singh, D., Aadhar, S., 2020b. Future exacerbation of hot and dry summer monsoon extremes in India. Npj Clim. Atmos. Sci. 3 (1), 1–9.
Mujumdar, M., et al., 2020. Droughts and floods. In: Krishnan, R., Sanjay, J., Gnanaseelan, C., Mujumdar, M., Kulkarni, A., Chakraborty, S. (Eds.), Assessment of Climate Change over the Indian Region. Springer, Singapore. https://doi.org/10.1007/978-981-15-4327-2_6.
Nagarajan, R., 2003. Drought: Assessment, Monitoring. Capital Publishing Company, Management and Resources Conservation.
Namias, J., Yuan, X., Cayan, D.R., 1988. Persistence of North Pacific Sea surface temperature and atmospheric flow patterns. J. Clim. 1 (7), 682–703.
Narasimhan, B., Srinivasan, R., 2005. Development and evaluation of Soil Moisture Deficit Index (SMDI) and Evapotranspiration Deficit Index (ETDI) for agricultural drought monitoring. Agric. For. Meteorol. 133 (1–4), 69–88.
Pai, D.S., Guhathakurta, P., Kulkarni, A., Rajeevan, M.N., 2017. Variability of meteorological droughts over India. In: Observed Climate Variability and Change over the Indian Region. Springer, Singapore, pp. 73–87.
Pal, J.S., Small, E.E., Eltahir, E.A.B., 2000. Simulation of regional-scale water and energy budgets Representation of subgrid cloud and precipitation processes within RegCM. J. Geophys. Res.: Atmos. 105(D24), 29579–29594.
Pant, M., Ghosh, S., Verma, S., Sinha, P., Mall, R.K., Bhatla, R., 2022. Simulation of an extreme rainfall event over Mumbai using a regional climate model: a case study. Meteorog. Atmos. Phys. 134 (1), 1–17.
Parthasarathy, B., Munot, A.A., Kothawale, D.R., 1994. All-India monthly and seasonal rainfall series: 1871–1993. Theor. Appl. Climatol. 49 (4), 217–224.
Paul, S., Ghosh, S., Oglesby, R., Pathak, A., Chandrasekharan, A., Ramsankaran, R.A.A.J., 2016. Weakening of Indian summer monsoon rainfall due to changes in land use land cover. Sci. Rep. 6 (1), 1–10.
Peterson, T.C., 2005. Climate change indices. WMO Bull. 54 (2), 83–86.

Pohl, B., Macron, C., Monerie, P.A., 2017. Fewer rainy days and more extreme rainfall by the end of the century in Southern Africa. Sci. Rep. 7 (1), 1–7.
Preethi, B., Ramya, R., Patwardhan, S.K., Mujumdar, M., Kripalani, R.H., 2019. Variability of Indian summer monsoon droughts in CMIP5 climate models. Clim. Dyn. 53 (3), 1937–1962.
Rajeevan, M., Bhate, J., 2009. A high resolution daily gridded rainfall dataset (1971–2005) for mesoscale meteorological studies. Curr. Sci. 558–562.
Rajeevan, M., Bhate, J., Jaswal, A.K., 2008. Analysis of variability and trends of extreme rainfall events over India using 104 years of gridded daily rainfall data. Geophys. Res. Lett. 35 (18).
Rajeevan, M., Gadgil, S., Bhate, J., 2010. Active and break spells of the Indian summer monsoon. J. Earth Syst. Sci. 119 (3), 229–247.
Raju, P.V.S., Bhatla, R., Almazroui, M., Assiri, M., 2015. Performance of convection schemes on the simulation of summer monsoon features over the South Asia CORDEX domain using RegCM-4.3. Int. J. Climatol. 35 (15), 4695–4706.
Ray, K., Pandey, P., Pandey, C., Dimri, A.P., Kishore, K., 2019. On the recent floods in India. Curr. Sci. 117 (2), 204–218.
Remedio, A.R., Teichmann, C., Buntemeyer, L., Sieck, K., Weber, T., Rechid, D., Hoffmann, P., Nam, C., Kotova, L., Jacob, D., 2019. Evaluation of new CORDEX simulations using an updated Köppen–Trewartha climate classification. Atmosphere 10 (11), 726. https://doi.org/10.3390/atmos10110726.
Roxy, M.K., Ritika, K., Terray, P., Murtugudde, R., Ashok, K., Goswami, B.N., 2015. Drying of Indian subcontinent by rapid Indian Ocean warming and a weakening land-sea thermal gradient. Nat. Commun. 6 (1), 1–10.
Roy, P.S., Roy, A., Joshi, P.K., Kale, M.P., Srivastava, V.K., Srivastava, S.K., Dwevidi, R. S., Joshi, C., Behera, M.D., Meiyappan, P., Sharma, Y., 2015. Development of decadal (1985–1995–2005) land use and land cover database for India. Remote Sens. 7 (3), 2401–2430.
Ruane, A.C., Teichmann, C., Arnell, N.W., Carter, T.R., Ebi, K.L., Frieler, K., Goodess, C. M., Hewitson, B., Horton, R., Kovats, R.S., Lotze, H.K., 2016. The vulnerability, impacts, adaptation and climate services advisory board (VIACS AB v1. 0) contribution to CMIP6. Geosci. Model Dev. 9 (9), 3493–3515.
Saeed, F., Hagemann, S., Jacob, D., 2012. A framework for the evaluation of the south Asian summer monsoon in a regional climate model applied to REMO. Int. J. Climatol. 32 (3), 430–440.
Sarojini, B.B., Stott, P.A., Black, E., 2016. Detection and attribution of human influence on regional precipitation. Nat. Clim. Chang. 6 (7), 669–675.
Shahi, N.K., Das, S., Ghosh, S., Maharana, P., Rai, S., 2021. Projected changes in the mean and intra-seasonal variability of the Indian summer monsoon in the RegCM CORDEX-CORE simulations under higher warming conditions. Clim. Dyn. 57 (5–6), 1489–1506.
Sikka, D.R., 1999. Monsoon drought in India. No. 2. Center for Ocean–Land–Atmosphere (COLA) Studies. Center for the Application of Research on the Environment.
Singh, S., Ghosh, S., Sahana, A.S., Vittal, H., Karmakar, S., 2017. Do dynamic regional models add value to the global model projections of Indian monsoon? Clim. Dyn. 48 (3), 1375–1397.
Sinha, P., Mohanty, U.C., Kar, S.C., Dash, S.K., Kumari, S., 2013. Sensitivity of the GCM driven summer monsoon simulations to cumulus parameterization schemes in nested RegCM3. Theor. Appl. Climatol. 112 (1), 285–306.
Solomon, S., Manning, M., Marquis, M., Qin, D., 2007. Climate Change 2007-the Physical Science Basis: Working Group I Contribution to the Fourth Assessment Report of the IPCC, vol. 4. Cambridge University Press.
Sørland, S.L., Brogli, R., Pothapakula, P.K., Russo, E., Van de Walle, J., Ahrens, B., Anders, I., Bucchignani, E., Davin, E.L., Demory, M.E., Dosio, A., 2021. COSMO-CLM regional climate simulations in the coordinated regional climate downscaling experiment (CORDEX) framework: a review. Geosci. Model Dev. 14 (8), 5125–5154.
Sperber, K.R., Annamalai, H., Kang, I.S., Kitoh, A., Moise, A., Turner, A., Wang, B., Zhou, T., 2013. The Asian summer monsoon: an intercomparison of CMIP5 vs. CMIP3 simulations of the late 20th century. Clim. Dyn. 41 (9–10), 2711–2744.
Svoboda, M.D., 2016. Essays on Decision Support for Drought Mitigation Planning: A Tale of Three Tools. The University of Nebraska-Lincoln.
Sylla, M.B., Giorgi, F., Pal, J.S., Gibba, P., Kebe, I., Nikiema, M., 2015. Projected changes in the annual cycle of high-intensity precipitation events over West Africa for the late twenty-first century. J. Clim. 28 (16), 6475–6488.
Tatli, H., Türkeş, M., 2011. Empirical orthogonal function analysis of the Palmer drought indices. Agric. For. Meteorol. 151 (7), 981–991.
Taylor, K.E., 2001. Summarizing multiple aspects of model performance in a single diagram. J. Geophys. Res.-Atmos. 106 (D7), 7183–7192.
The Hindu, 2019. https://www.thehindu.com/news/national/36-million-indians-face-flood-risk-study/article29825978.ece.
Tiedtke, M., 1989. A comprehensive mass flux scheme for cumulus parameterization in large-scale models. Mon. Weather Rev. 117(8), 1779–1800.
Trenberth, K.E., 2011. Changes in precipitation with climate change. Clim. Res. 47 (1–2), 123–138.
Trenberth, K.E., Dai, A., Rasmussen, R.M., Parsons, D.B., 2003. The changing character of precipitation. Bull. Am. Meteorol. Soc. 84 (9), 1205–1218.
Tsakiris, G., 2017. Drought risk assessment and management. Water Resour. Manag. 31 (10), 3083–3095.
Varikoden, H., Revadekar, J.V., 2020. On the extreme rainfall events during the southwest monsoon season in northeast regions of the Indian subcontinent. Meteorol. Appl. 27 (1), e1822.
Vasiliades, L., Loukas, A., Liberis, N., 2011. A water balance derived drought index for Pinios River Basin, Greece. Water Resour. Manag. 25 (4), 1087–1101.
Verma, S., Bhatla, R., 2021. Performance of RegCM4 for dynamically downscaling of El Nino/La Nina events during southwest monsoon over India and its regions. Earth Space Sci. 8 (3), e2020EA001474.
Verma, S., Bhatla, R., Ghosh, S., Sinha, P., Mall, R.K., Pant, M., 2021. Spatio-temporal variability of summer monsoon surface air temperature over India and its regions using regional climate model. Int. J. Climatol. 41 (13), 5820–5842. https://doi.org/10.1002/joc.7155.
Zhao, Y., Zhang, H., 2016. Impacts of SST warming in tropical Indian Ocean on CMIP5 model-projected summer rainfall changes over Central Asia. Clim. Dyn. 46 (9), 3223–3238.
Zhu, H., Jiang, Z., Li, J., Li, W., Sun, C., Li, L., 2020. Does CMIP6 inspire more confidence in simulating climate extremes over China? Adv. Atmos. Sci. 37 (10), 1119–1132.
Zolina, O., Simmer, C., Belyaev, K., Gulev, S.K., Koltermann, P., 2013. Changes in the duration of European wet and dry spells during the last 60 years. J. Clim. 26 (6), 2022–2047.